

Electronic Supplementary Information for Understanding Differences in Rate versus Product Determining Steps to Enhance Sequence Control in Epoxide/Cyclic Anhydride Copolymers

Zachary A. Wood,^a and Megan E. Fieser^{*a,b}

^aDepartment of Chemistry, University of Southern California, Los Angeles, California 90089

^bWrigley Institute for Environmental Studies, University of Southern California, Los Angeles, California, 90089

1. General Considerations	S4
2. General Procedures for Polymerization	S5
2.1 General Procedure for Anhydride Reactivity Ratio Reactions	S5
3. Kinetics procedures	S6
3.1 ^1H NMR Kinetics Procedure	S6
Table S1 Experimental data for kinetic polymerization experiments	S6
Fig. S1 Example of CHO/CPMA stack used for ^1H NMR kinetics	S7
3.2 Initial Rate Determination	S7
Fig. S2 Example of plot used for to obtain an initial rate from kinetic studies	S8
Table S2 Determined orders for CHO, CPMA, and Cat	S8
3.3 COPASI Fitting Software	S8
Fig. S3 COPASI fit for Table S1, Entry 1d.	S9
4. Tabulated Polymerization Data	S10
Table S3 Tabulated polymerization data for ROCOP of CHO, BO, and CPMA catalyzed by $\text{YCl}_3 \cdot 6\text{H}_2\text{O}/[\text{PPN}]\text{Cl}$.	S10
Table S4 Tabulated polymerization data for ROCOP of CHO, and multiple anhydrides, catalyzed by $\text{YCl}_3 \cdot 6\text{H}_2\text{O}/[\text{PPN}]\text{Cl}$	S10
5. ^1H NMR Spectra of Isolated Polymers and Reaction Mixtures	S11
5.1 ^1H NMR of Polymerization Reactions	S11
Fig. S4 ^1H NMR spectrum of CHO/CPMA- <i>r</i> -BO/CPMA in CDCl_3 (Table 2, Entry 1).	S11
Fig. S5 ^1H DOSY NMR spectrum of CHO/CPMA- <i>r</i> -BO/CPMA (Table 2, Entry 1)	S12
Fig. S6 ^1H NMR spectrum stack of BO/CPMA, CHO/CPMA, and CHO/CPMA- <i>r</i> -BO/CPMA (Table 2, Entry 1)	S13
Fig. S7 ^1H NMR spectrum stack of timepoints for CHO/PA- <i>r</i> -BO/PA	S14
Fig. S8 ^1H NMR spectrum stack of timepoints for CHO/PA- <i>r</i> -BO/PA	S15
Fig. S9 ^1H NMR spectrum of CHO/CPMA- <i>r</i> -BO/CPMA in CDCl_3 (Table 2, Entry 2)	S16

Fig. S10 ^1H NMR spectrum of CHO/CPMA- <i>r</i> -BO/CPMA in CDCl_3 (Table 2, Entry 3)	S17
Fig. S11 ^1H NMR spectrum of CHO/CPMA- <i>r</i> -BO/CPMA in CDCl_3 (Table 2, Entry 4)	S18
Fig. S12 ^1H NMR spectrum of CHO/CPMA- <i>r</i> -BO/CPMA in CDCl_3 (Table 2, Entry 5)	S19
Fig. S13 ^1H NMR spectra of CHO/PA- <i>b</i> -CHO/CPMA monitored at 110 °C (Fig. 3b)	S20
Fig. S14 ^1H NMR spectra of CHO/PA- <i>b</i> -CHO/CPMA in CDCl_3 monitored by aliquots	S21
Fig. S15 ^1H NMR spectra of BO/PA- <i>b</i> -BO/CPMA in CDCl_3 monitored by aliquots	S22
Fig. S16 ^1H NMR spectra of aliquots for CHO/PA- <i>b</i> -CHO/CPMA in CDCl_3 (Table S4, Entry 1).	S23
Fig. S17 ^1H NMR of CHO/PA- <i>b</i> -CHO/CPMA in CDCl_3 (Table S4, Entry 1)	S24
Fig. S18 ^1H NMR of CHO/PA- <i>b</i> -CHO/CPMA in CDCl_3 (Table S4, Entry 2)	S25
Fig. S19 ^1H DOSY of CHO/PA- <i>b</i> -CHO/CPMA in CDCl_3 (Table S4, Entry 2).	S26
Fig. S20 ^1H NMR spectra of CHO/GA- <i>r</i> -CHO/CPMA monitored at 110 °C (Fig. 3c)	S27
Fig. S21 ^1H NMR spectra of CHO/GA- <i>r</i> -CHO/CPMA in CDCl_3 monitored by aliquots.	S28
Fig. S22 ^1H NMR spectrum of CHO/GA- <i>r</i> -CHO/CPMA in CDCl_3 (Table S4, Entry 3).	S29
Fig. S23 ^1H NMR spectra stack of CHO/GA- <i>r</i> -CHO/CPMA in CDCl_3 (Table S4, Entry 3).	S30
Fig. S24 ^1H NMR of CHO/GA- <i>r</i> -CHO/CPMA in CDCl_3 (Table S4, Entry 4).	S31
Fig. S25 ^1H NMR spectra stack of CHO/GA- <i>r</i> -CHO/CPMA in CDCl_3 (Table S4, Entry 4).	S32
Fig. S26 ^1H NMR of CHO/GA- <i>r</i> -CHO/CPMA in CDCl_3 (Table S4, Entry 5).	S33
Fig. S27. ^1H NMR spectra stack of CHO/GA- <i>r</i> -CHO/CPMA in CDCl_3 (Table S4, Entry 5). Aliquots taken at 30 min, 1 hr, 1.5 hr, and 4 hr.	S34
Fig. S28 ^1H DOSY of CHO/GA- <i>r</i> -CHO/CPMA in CDCl_3 (Table S4, Entry 5)	S35
Fig. S29 ^1H NMR of CHO/PA- <i>r</i> -CHO/GA in CDCl_3 (Table S4, Entry 6)	S36
Fig. S30 ^1H DOSY of CHO/PA- <i>r</i> -CHO/GA in CDCl_3 (Table S4, Entry 6).	S37
Fig. S31 ^1H NMR spectra stack of CHO/GA- <i>r</i> -CHO/CPMA in CDCl_3 (Table S4, Entry 6)	S38
5.2 Anhydride ring-opening studies	S39
Fig. S32 ^1H NMR analysis of aliquots from the reaction of GA and CPMA with 100 equivalents of MeOH	S39
Fig. S33 ^1H NMR analysis of aliquots from the reaction of PA and CPMA with 100 equivalents of MeOH	S40
6 GPC Data	S41
Fig. S34 GPC trace corresponding to Table 2, Entry 1	S41
Fig. S35 GPC traces (MALS detector left, RI detector right) corresponding to Table 2, Entry 2	S41
Fig. S36 GPC trace corresponding to Table 2, Entry 3	S42
Fig. S37 GPC trace corresponding to Table 2, Entry 4	S42
Fig. S38 GPC trace corresponding to Table 2, Entry 5	S43
Fig. S39 GPC trace corresponding to Table S3, Entry 1	S43
Fig. S40 GPC trace corresponding to Table S3, Entry 7	S44
Fig. S41 GPC trace corresponding to Table S4, Entry 3	S44
Fig. S42 GPC trace corresponding to Table S4, Entry 4	S45

Fig. S43	GPC trace corresponding to Table S4, Entry 5	S45
Fig. S44	GPC trace corresponding to Table S4, Entry 1	S46
Fig. S45	GPC trace corresponding to Table S4, Entry 2	S46
Fig. S46	GPC trace corresponding to Table S4, Entry 6	S47
7	Differential Scanning Calorimetry Data	S47
Fig. S47	DSC trace of CHO/CPMA- <i>r</i> -BO/CPMA from Table 2, Entry 1	S48
Fig. S48	DSC trace of CHO/CPMA- <i>r</i> -BO/CPMA from Table 2, Entry 2	S48
Fig. S49	DSC trace of CHO/CPMA- <i>r</i> -BO/CPMA from Table 2, Entry 3.	S49
Fig. S50	DSC trace of CHO/CPMA- <i>r</i> -BO/CPMA from Table 2, Entry 4	S49
Fig. S51	DSC trace of CHO/CPMA- <i>r</i> -BO/CPMA from Table 2, Entry 5.	S50
Fig. S52	DSC trace of BO/CPMA from Table S4, Entry 1	S50
Fig. S53	DSC trace of CHO/CPMA from Table S4, Entry 7	S51
Fig. S54	DSC trace of CHO/PA- <i>b</i> -CHO/CPMA from Table S5, Entry 1	S51
Fig. S55	DSC trace of CHO/PA- <i>b</i> -CHO/CPMA from Table S5, Entry 2	S52
Fig. S56	DSC trace of CHO/GA- <i>r</i> -CHO/CPMA from Table S5, Entry 3	S52
Fig. S57	DSC trace of CHO/GA- <i>r</i> -CHO/CPMA from Table S5, Entry 4	S53
Fig. S58	DSC trace of CHO/GA- <i>r</i> -CHO/CPMA from Table S5, Entry 5	S53
Fig. S58	DSC trace of CHO/GA- <i>r</i> -CHO/CPMA from Table S5, Entry 5	S54
8	Reactivity Ratios	S55
8.1	Calculation of Reactivity Ratios	S55
8.2	Additional reactivity ratio plots	S55
Fig. S60	Plot of CHO/PA/GA and CHO/PA/CPMA	S55
Fig. S61	Plot of % incorporation of CHO/GA vs. CHO/CPMA	S56
8.3	Data for Epoxide Mixtures	S57
Fig. S62	Plot of CHO and BO conversion vs. total epoxide conversion	S57
9	References	S58

1. General Considerations

All polymerization reactions were set up on a benchtop under atmospheric conditions. Protio and deuterated chloroform were purchased from commercial suppliers and used as received. 1-Butene oxide (BO) and cyclohexene oxide (CHO) were dried over CaH₂, degassed by three freeze-pump-thaw cycles and vacuum transferred prior to use, unless stated otherwise. Carbic anhydride (CPMA) was recrystallized from hot 30:70 ethyl acetate/hexanes and dried under reduced pressure for 24 h prior to use. Phthalic anhydride (PA) was sublimed prior to use. Glutaric anhydride (GA) was purchased from commercial suppliers and used as received. Bis(triphenylphosphine)iminium chloride ([PPN]Cl) was recrystallized from CH₂Cl₂/hexanes and dried under reduced pressure for 24 h prior to use.

Methods. ¹H NMR spectra were recorded on a Varian 400-MR 2-Channel, Varian Mercury 400 2-Channel, Varian VNMRS-500 2-Channel, and Varian VNMRS-600 3-Channel NMR spectrometers and referenced against residual protio solvent resonances. ¹H NMR kinetics were recorded on a Varian VNMRS-600 3-Channel NMR spectrometer. Polymer molecular weights and dispersities were determined using a SEC-MALS instrument equipped with an Agilent 1260 Infinity II HPLC System and autosampler, 2 Agilent PolyPore columns (both 5 micron, 4.6 mm ID) in sequence, a Wyatt DAWN HELEOS-II light scattering detector, and a Wyatt Optilab T-rEX refractive index detector. The columns were eluted with HPLC grade THF at 30 °C at a flow rate of 0.3 mL/min, and polymer samples were dissolved in this solvent and filtered through a 0.2 micron PTFE membrane before dRI analyses. dn/dc values were calculated from the RI signal by using the 100% mass recovery method in the Astra software and a known sample concentration. The DSC measurements were made at a heating rate of 10 °C/min and N₂ flow rate of 20 ml/min, and T_g values were obtained from the midpoint of the glass transition in the second heating curve. DSC traces were recorded using a Perkin-Elmer DSC 8000 and processed with Pyris software.

2. General Procedures for Polymerization

On the benchtop, $\text{YCl}_3 \cdot 6\text{H}_2\text{O}$ (1 equiv), [PPN]Cl (1 equiv), anhydride, epoxide and a stir bar were charged into a vial equipped with a Teflon-lined cap. For epoxide mixtures (Table S3), $\text{YCl}_3 \cdot 6\text{H}_2\text{O}$ (1 equiv, 3.3 mg, 0.011 mmol), [PPN]Cl (1 equiv, 6.2 mg, 0.011 mmol), carbic anhydride (400 equiv, 702.0 mg, 4.2 mmol), and a total of 2 mL of epoxides were added to the vial. For anhydride mixtures (Table S4), $\text{YCl}_3 \cdot 6\text{H}_2\text{O}$ (1 equiv, 3.0 mg, 0.0099 mmol), [PPN]Cl (1 equiv, 5.7 mg, 0.0099 mmol), cyclohexene oxide (2000 equiv, 2 mL, 19.7 mmol), and two anhydrides of choice (200 equiv. each, 1.97 mmol) were added to the vial. The vial was then taped with electrical tape, and placed inside a Chemglass high throughput tray that was preheated to 110 °C for at least 1 h. After the desired time, the vial was cooled to room temperature and the resulting mixture was dissolved in 1 mL of chloroform. Hexanes was then added in excess until the polymer started to precipitate out. The precipitate was allowed to settle, and the supernatant was pipette away. The isolated polymer was then dried under reduced pressure at 110 °C overnight. Conversions were calculated via analysis of crude ^1H NMR spectra in CDCl_3 .

2.1 General Procedure for Anhydride Reactivity Ratio Reactions

On the benchtop, $\text{YCl}_3 \cdot 6\text{H}_2\text{O}$ (1 equiv, 3.0 mg, 0.0099 mmol), [PPN]Cl (1 equiv, 5.7 mg, 0.0099 mmol), 2 anhydrides of choice (each 50 equiv, 0.49 mmol), cyclohexane oxide (500 equiv, 0.50 mL, 4.94 mmol) and a stir bar were charged into a vial equipped with a Teflon-lined cap and placed inside a Chemglass high throughput tray that was preheated to the desired reaction temperature (80 °C or 110 °C) for at least 1 h. Aliquots, which were then dissolved in CDCl_3 , were then taken at selected times for each reaction to monitor monomer conversion by ^1H NMR (Fig. 5 and Fig. S60).

3. Kinetics Procedure

3.1 ^1H NMR Kinetics Procedures. A representative procedure for the kinetic studies is described and adopted from Tolman and coworkers.¹ Catalyst, cocatalyst, and anhydride were weighed into a glass vial with a Teflon coated cap on the benchtop. The epoxide was added via syringe and the vial was stirred at 60 °C for 5 minutes. In cases with lower epoxide concentrations, chlorobenzene was added to keep the total volume between 700 and 780 μL . The final volume of each homogenous solution was measured with a syringe, and the solution was immediately transferred to a oven-dried NMR tube containing a 15.7 mM capillary solution of p-C₆H₄(TMS)₂ in C₆D₆. The NMR tube was capped, the cap wrapped in electrical tape and the tube was transferred to a spectrometer. The temperature of the NMR spectrometer was calibrated to 110 °C using a pure ethylene glycol standard. An arrayed set of spectra were taken with no delay between each, with 8 scans and maximum gain. The arrayed experiment was allowed to proceed until >20% of anhydride was consumed unless otherwise noted. The obtained arrayed NMR data were phased and baseline corrected in Mestrenova before being integrated in the same program. The integrations were recorded and entered into an Excel spreadsheet. Absolute concentrations of epoxide and anhydride as a function of time were computed relative to the concentration of the internal standard.

Table S1. Experimental data for kinetic polymerization experiments.

Condition #	[YCl ₃ ·6H ₂ O] (M) ^a	[PPN]Cl] (M) ^a	[CHO] (M) ^b	[CPMA] (M) ^b	Initial rate (M/s) ^c
1a	0.016	0.017	9.10	1.76	6.8x10 ⁻⁴
1b	0.016	0.017	10.50	2.02	8.0x10 ⁻⁴
1c	0.016	0.017	8.83	1.77	1.3x10 ⁻³
1d	0.016	0.016	12.24	2.36	1.6x10 ⁻³
2a	0.019	0.020	10.52	1.57	1.0x10 ⁻³
3a	0.019	0.020	11.69	1.18	1.4x10 ⁻³
4a	0.021	0.020	7.07	1.84	7.7x10 ⁻⁴
5a	0.021	0.019	3.93	1.41	3.1x10 ⁻⁴

^a Calculated concentrations from weight of material and final volumes of the reaction solution. ^b Observed concentration in ^1H NMR, calibrated with the internal standards. ^c Initial rates described in section 3.2.

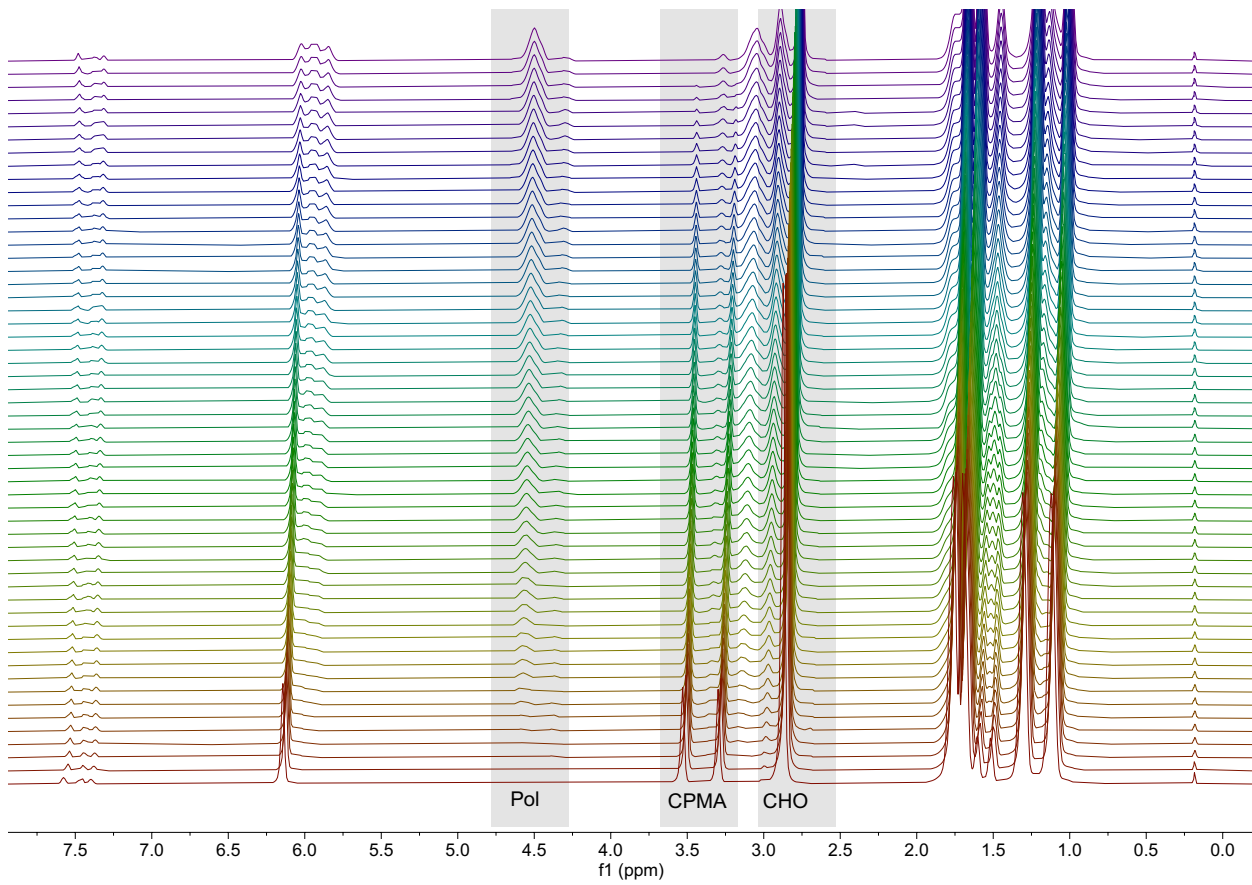


Fig. S1 Example of CHO/CPMA stack used for ^1H NMR kinetics.

3.2 Initial Rate Determination. Reaction orders were determined by examining initial rates of reaction. Due to the varying times taken to set up each run, one particular time point could not be used be used for comparison between reactions. The concentration of polymer vs. time data was fit to a first order polynomial (Fig. S2). Using the linear fit, reaction times at 15% completion, determined by examining the amount of anhydride reacted, were compared. An order was determined for every combination of runs using eq 1, where the rate constant, k , and conditions with identical conditions cancel, and averaged. Table S2 shows a summary of the determined orders.

$$\frac{\text{Rate}_1}{\text{Rate}_2} = \frac{k[\text{CHO}]_1^x[\text{CPMA}_1]^y[\text{Cat}_1]^z}{k[\text{CHO}_2]^x[\text{CPMA}_2]^y[\text{Cat}_2]^z} \quad (1)$$

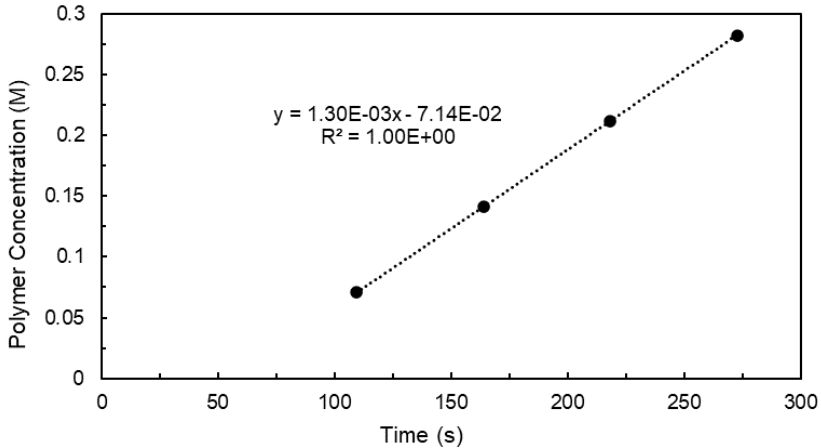


Figure S2 Example of plot used for to obtain an initial rate from kinetic studies.

Table S2. Determined orders for CHO, CPMA, and Cat ($\text{YCl}_3 \cdot 6\text{H}_2\text{O}/[\text{PPN}]\text{Cl}$ pair) using initial rates.

	CHO	CPMA
Reaction order	0.9 (4)	0.0 (6)

3.3 COPASI Fitting Software. The concentration vs time data obtained from the ^1H NMR data were input into the global kinetics fitting program COPASI (version 4.30), and fit to eq 2 to obtain a k_{obs} value.²

$$\text{Rate} = k_{\text{obs}}[\text{CHO}] \quad (2)$$

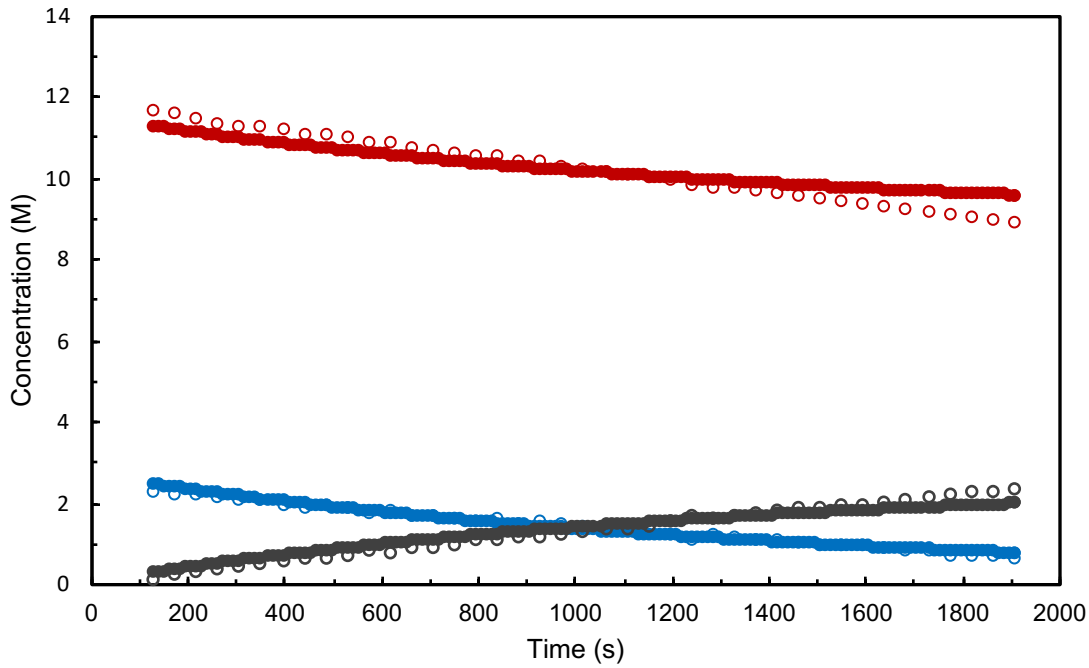


Fig. S3 COPASI fit for Table S1, Entry 1d. Colored circles represent experimental data, and the solid lines represent the fit data for each species. $K_{\text{obs}} = 6.57 \times 10^{-5} \text{ (1)} (\text{M s}^{-1})$

4. Tabulated polymerization data

Table S3. Tabulated polymerization data for ROCOP of CHO, BO, and CPMA catalyzed by $\text{YCl}_3 \cdot 6\text{H}_2\text{O}/[\text{PPN}]\text{Cl}$.^a

Entry #	$f_{\text{BO}}:f_{\text{CHO}}$	$F_{\text{BO}}:F_{\text{CHO}}$ (expt.)	% conversion ^d	% ester ^e	% epimer ^f	ExpM_n (kDa) ^g	D^g	T_g^h (°C)
1	2000:0	100:0	73	97	14	4.9	1.49	54
2	1600:400	79:21	85	>99	8	4.5	1.18	69
3	1200:800	65:35	81	>99	11	3.8	1.26	79
4	1000:1000	48:52	76	98	8	4.1	1.24	91
5	800:1200	37:63	79	99	5	3.7	1.27	99
6	400:1600	28:72	66	97	13	3.2	1.23	97
7	0:2000	0:100	60	98	9	3.1	1.23	116

^a [BO+CHO]:[CPMA]:[$\text{YCl}_3 \cdot 6\text{H}_2\text{O}$]:[[PPN]Cl] was 1908 - 2091:400:1:1 at 110 °C for 4 hrs. ^b Ratios are in μL to keep a consistent volume, with 2 mL epoxide used. ^c Based on 1H NMR of the purified polymers, comparing polyester BO peaks to polyester CHO peaks. ^d Determined using 1H NMR spectra of crude reaction mixtures, comparing conversion of anhydride to polymer. ^e Based on 1H NMR of the purified polymers, comparing the polyether signal to the polyester signal. ^f Determined using 1H NMR spectra of purified polymers as described previously: epim (%) = {2 x A2.7 ppm/(6.0-6.5)} x 100.³ ^g Identified by gel permeation chromatography (GPC), using a Wyatt dRI detector calibrated with polystyrene standards. ^h Determined by differential scanning calorimetry (DSC).

Table S4. Tabulated polymerization data for ROCOP of CHO, and multiple anhydrides, catalyzed by $\text{YCl}_3 \cdot 6\text{H}_2\text{O}/[\text{PPN}]\text{Cl}$.^a

Entry #	Anhydride equiv.	% conversion ^b	% ester ^c	% epimer ^d	ExpM_n (kDa) ^e	D^e	T_g^f (°C)
1	300CPMA:100PA	66,>99	92	15	3.3	1.21	121
2	200CPMA:200PA	>99,>99	82	16	3.5	1.21	125
3	300CPMA:100GA	83,>99	90	25	2.2	1.43	87
4	200CPMA:200GA	>99,>99	83	27	2.2	1.57	60
5	100CPMA:300GA	>99,>99	71	50	2.1	1.63	34
6	200PA:200GA	>99,>99	74	-	1.6	1.56	55

^a [CHO]:[Anhydride A + Anhydride B]:[$\text{YCl}_3 \cdot 6\text{H}_2\text{O}$]:[[PPN]Cl] was 2000:400:1:1 at 110 °C for 4 hrs. ^b Determined using 1H NMR spectra of crude reaction mixtures, comparing conversion of anhydride to polymer. ^c Based on 1H NMR of the purified polymers, comparing polyester BO peaks to polyester CHO peaks. ^d Based on 1H NMR of the purified polymers, comparing the polyether signal to the polyester signal. ^e Determined using 1H NMR spectra of purified polymers as described previously: epim (%) = {2 x A2.7 ppm/(6.0-6.5)} x 100.³ ^f Identified by gel permeation chromatography (GPC), using a Wyatt dRI detector calibrated with polystyrene standards.

^f Determined by differential scanning calorimetry (DSC).

5. ^1H NMR Spectra of Isolated Polymers and Reaction Mixtures

5.1 ^1H NMR Spectra from Polymerization Reactions

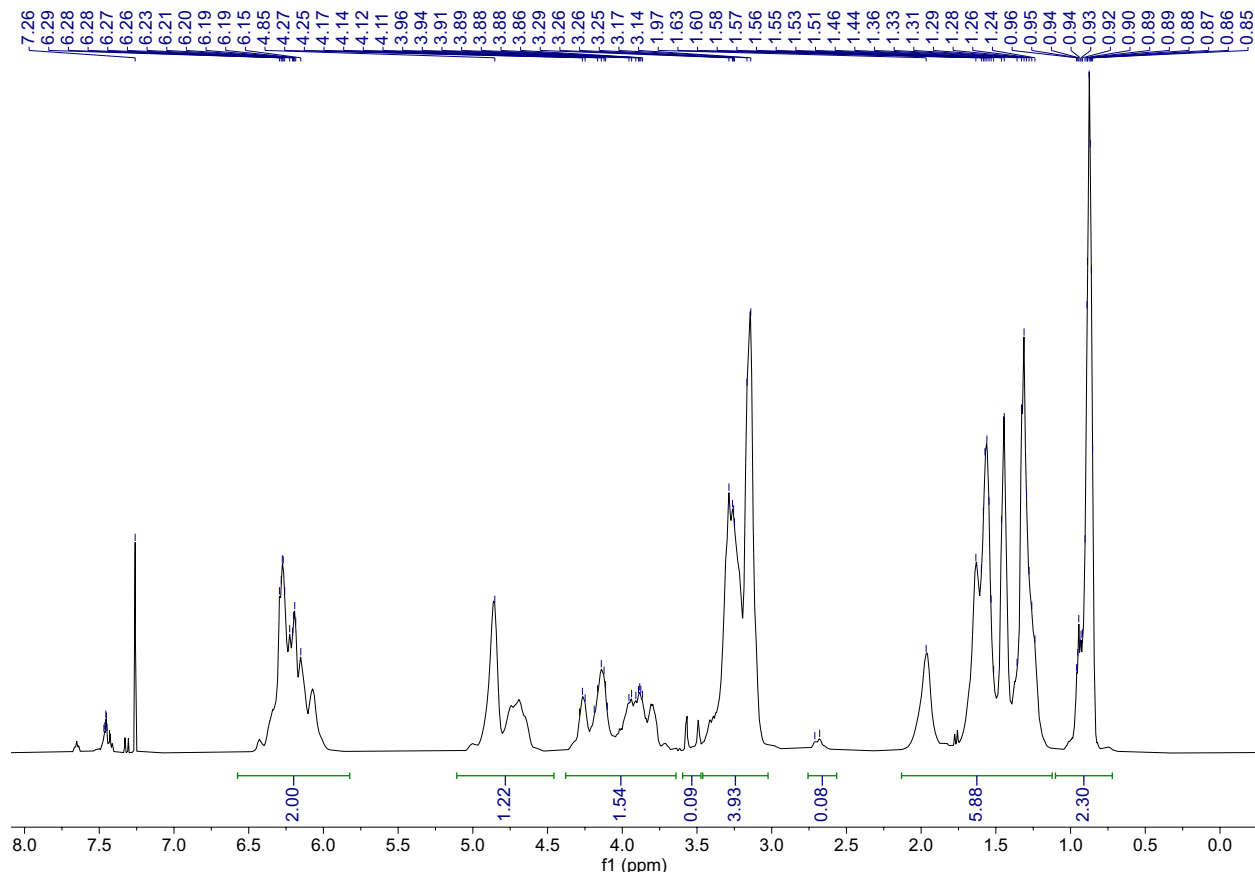


Fig. S4 ^1H NMR spectrum of CHO/CPMA-*r*-BO/CPMA in CDCl_3 (Table 2, Entry 1). Resonances > 7.26 ppm assignable to [PPN] phenyl groups (from the [PPN]Cl).

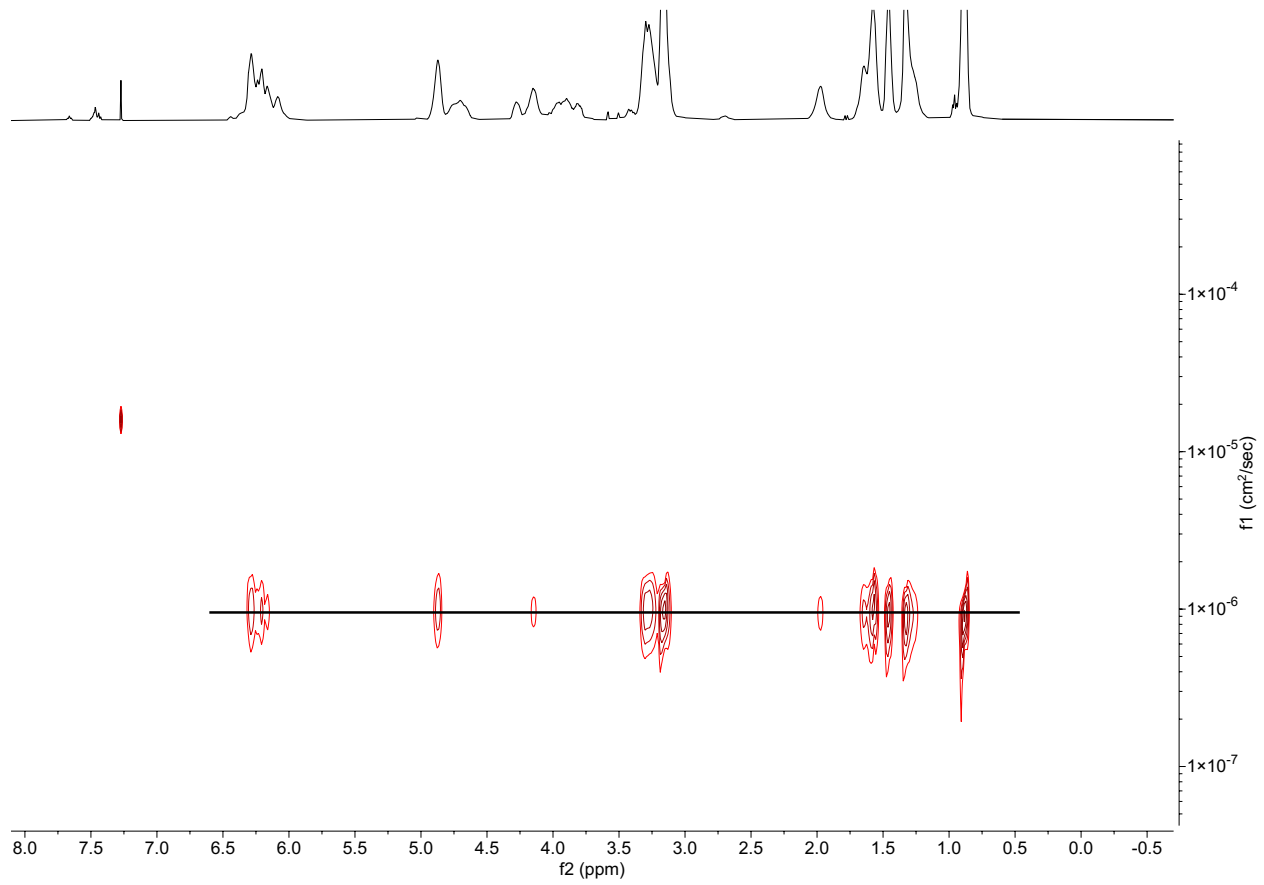


Fig. S5 ¹H DOSY NMR spectrum of CHO/CPMA-*r*-BO/CPMA in CDCl₃ (Table 2, Entry 1).

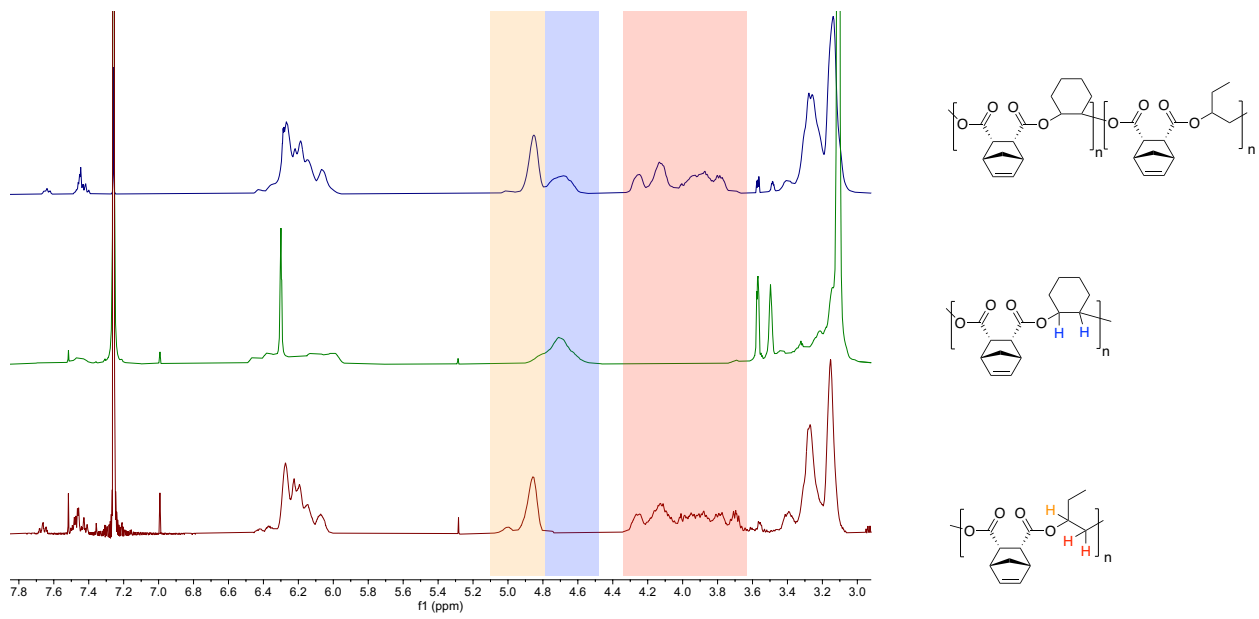


Fig. S6 ^1H NMR spectrum stack of BO/CPMA, CHO/CPMA, and CHO/CPMA-*r*-BO/CPMA in CDCl_3 (Table 2, Entry 1).

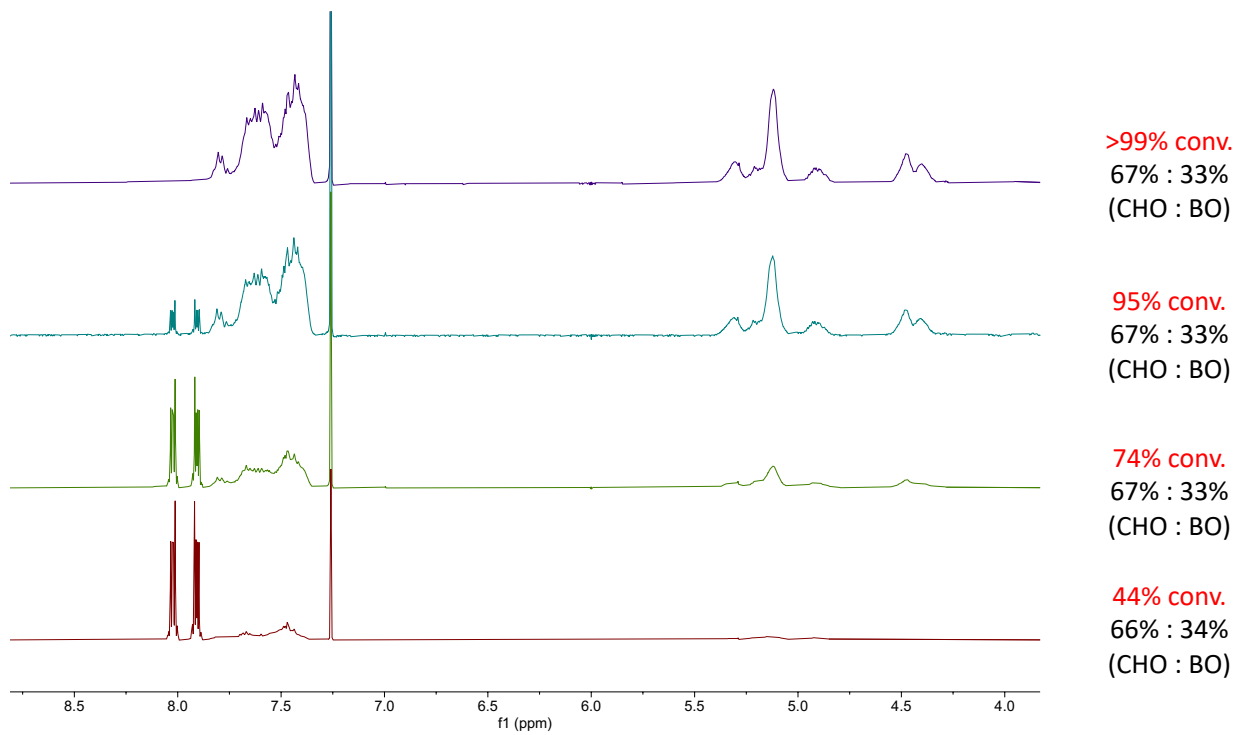
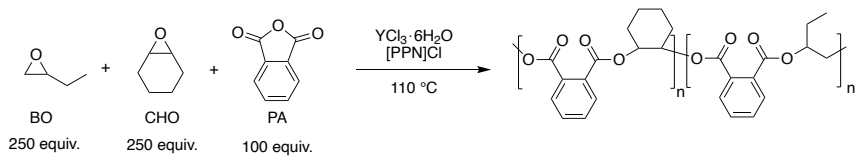


Fig. S7 ^1H NMR spectrum stack of timepoints for CHO/PA-*r*-BO/PA in CDCl_3 . % conversion of PA is in red.

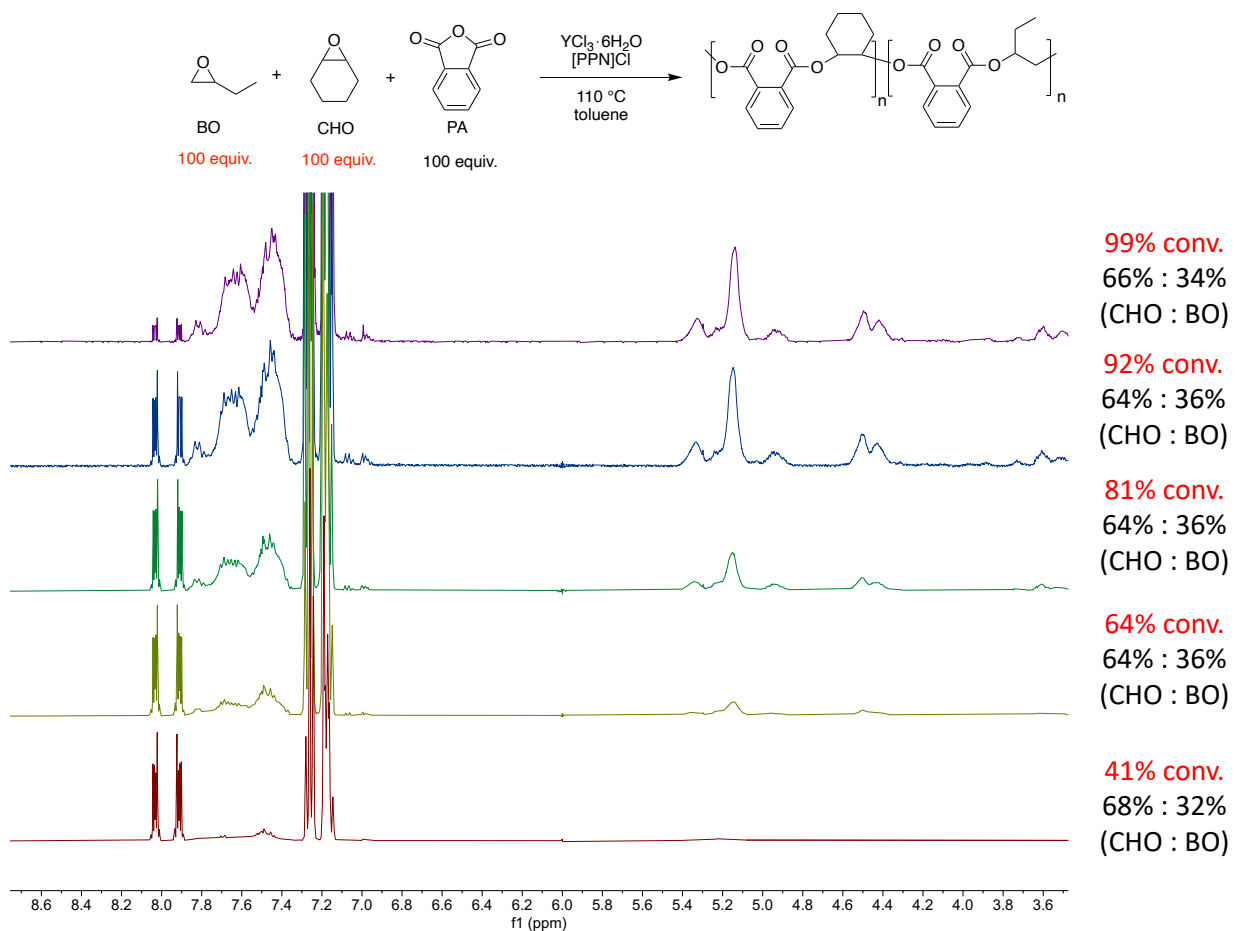


Fig. S8 ^1H NMR spectrum stack of timepoints for CHO/PA-*r*-BO/PA in CDCl_3 . % conversion of PA is in red.

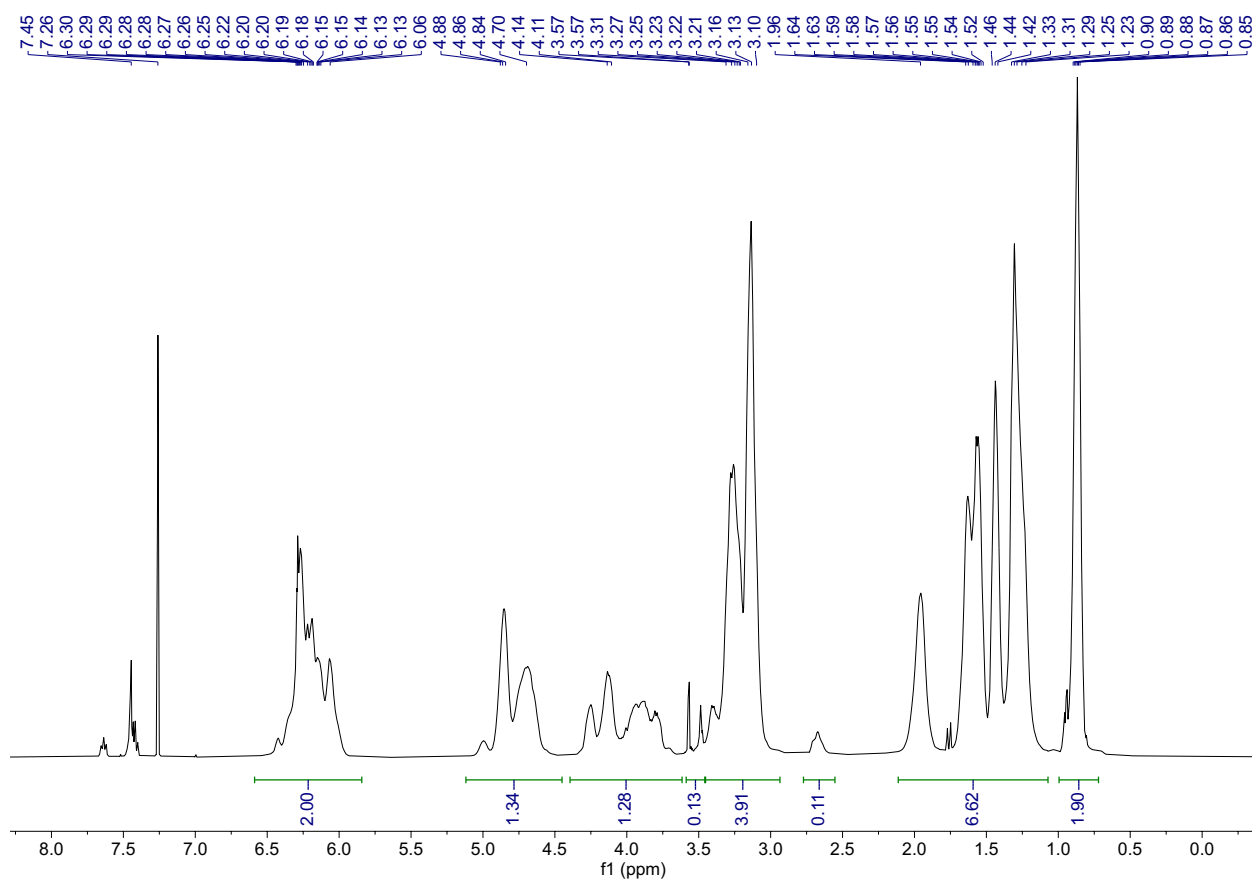


Fig. S9 ^1H NMR spectrum of CHO/CPMA-*r*-BO/CPMA in CDCl_3 (Table 2, Entry 2). Resonances > 7.26 ppm assignable to [PPN] phenyl groups.

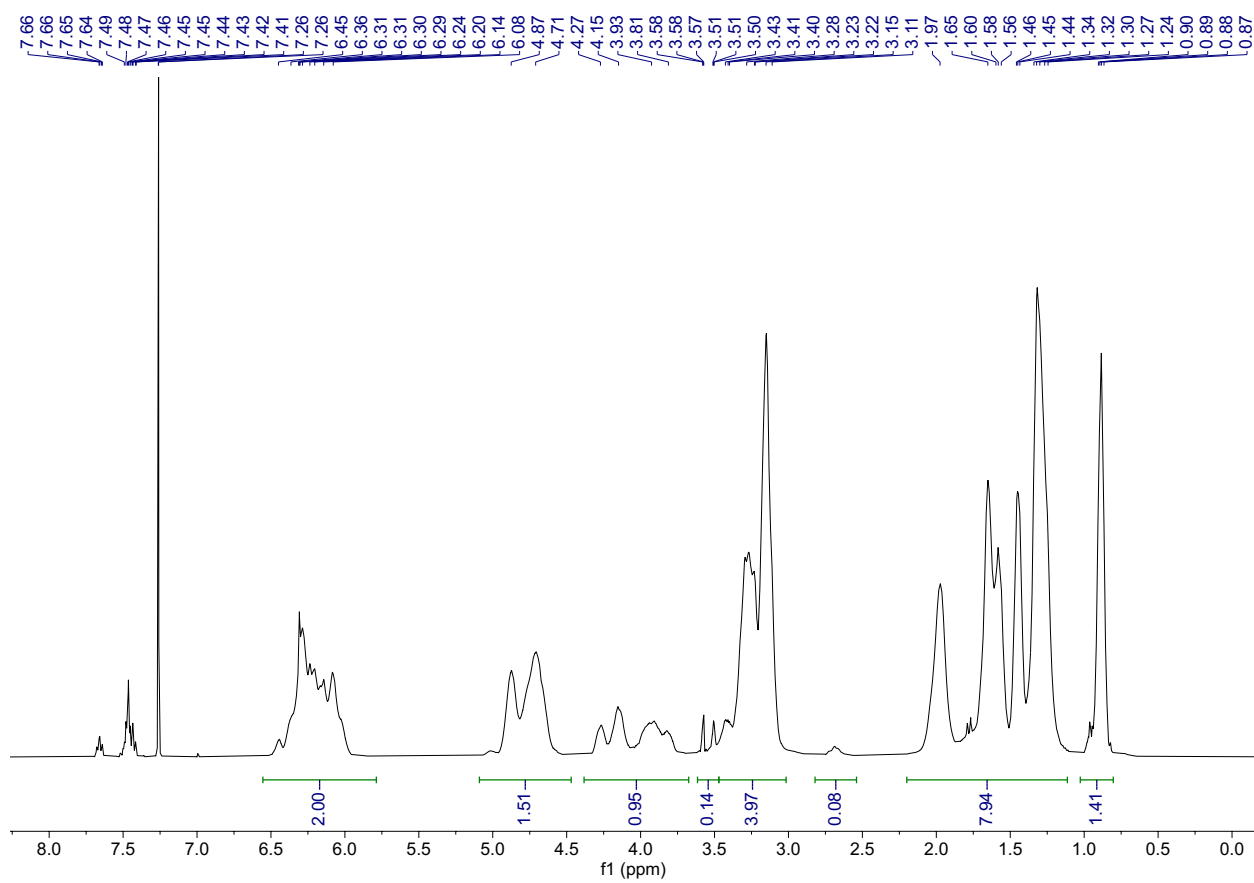


Fig. S10 ^1H NMR spectrum of CHO/CPMA-*r*-BO/CPMA in CDCl_3 (Table 2, Entry 3). Resonances > 7.26 ppm assignable to PPN phenyl groups.

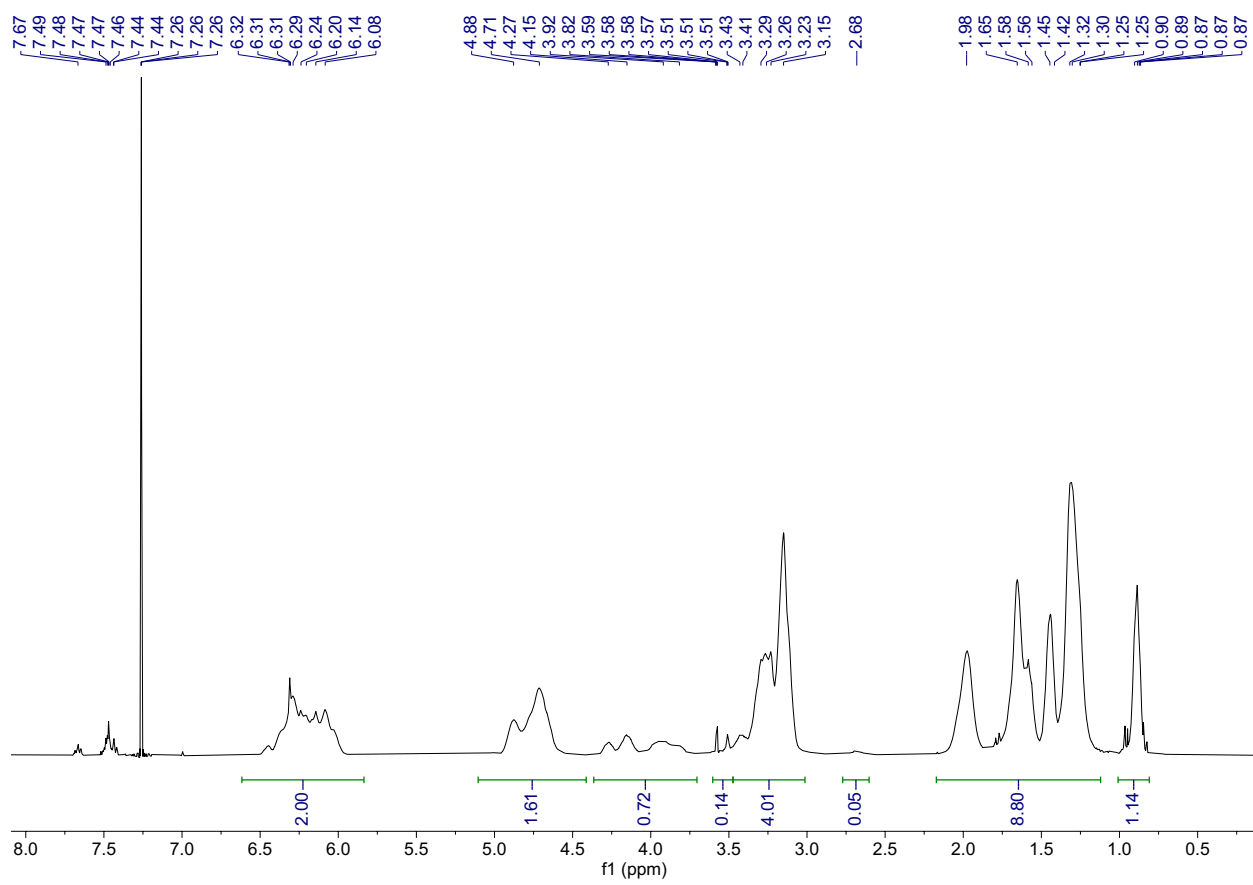


Fig. S11 ^1H NMR spectrum of CHO/CPMA-*r*-BO/CPMA in CDCl_3 (Table 2, Entry 4). Resonances > 7.26 ppm assignable to PPN phenyl groups.

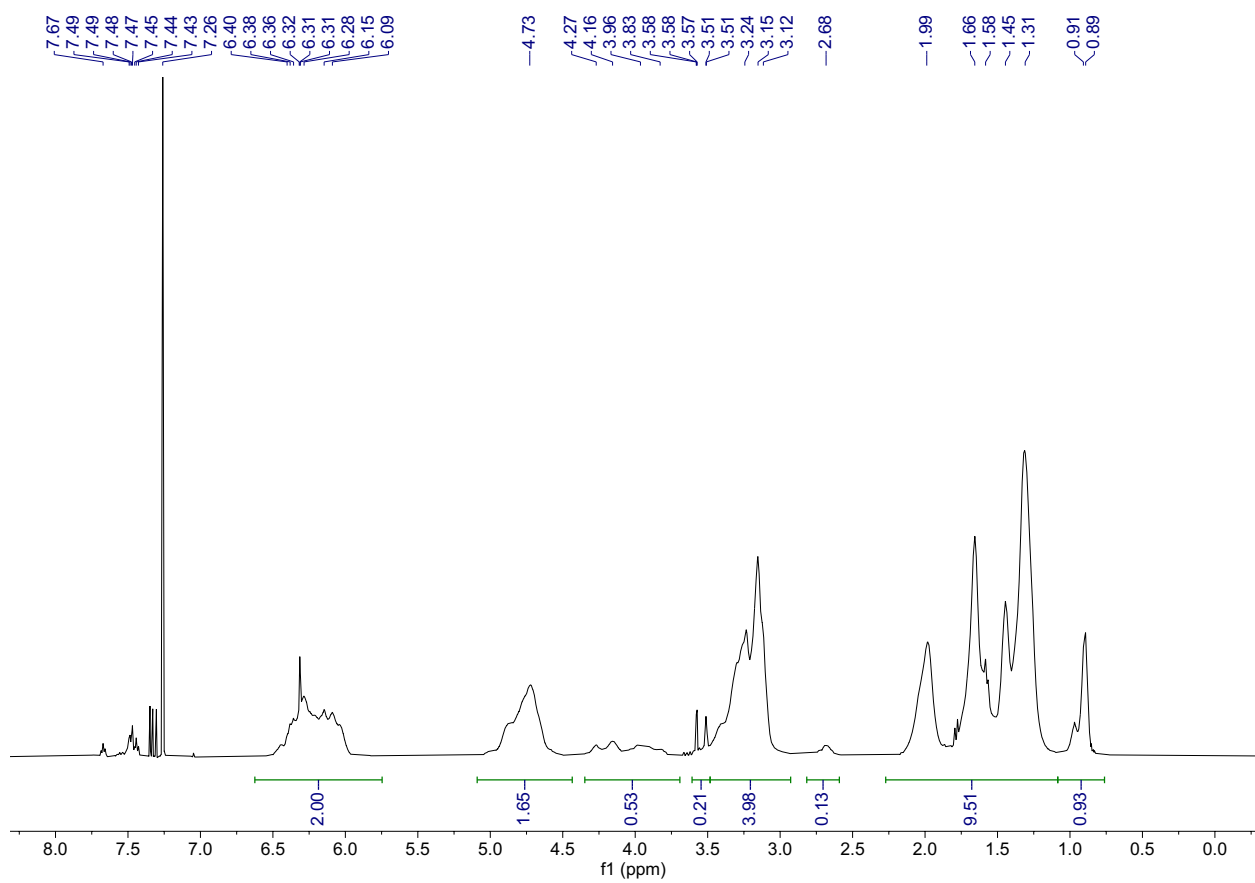


Fig. S12 ¹H NMR spectrum of CHO/CPMA-*r*-BO/CPMA in CDCl₃ (Table 2, Entry 5). Resonances > 7.26 ppm assignable to PPN phenyl groups.

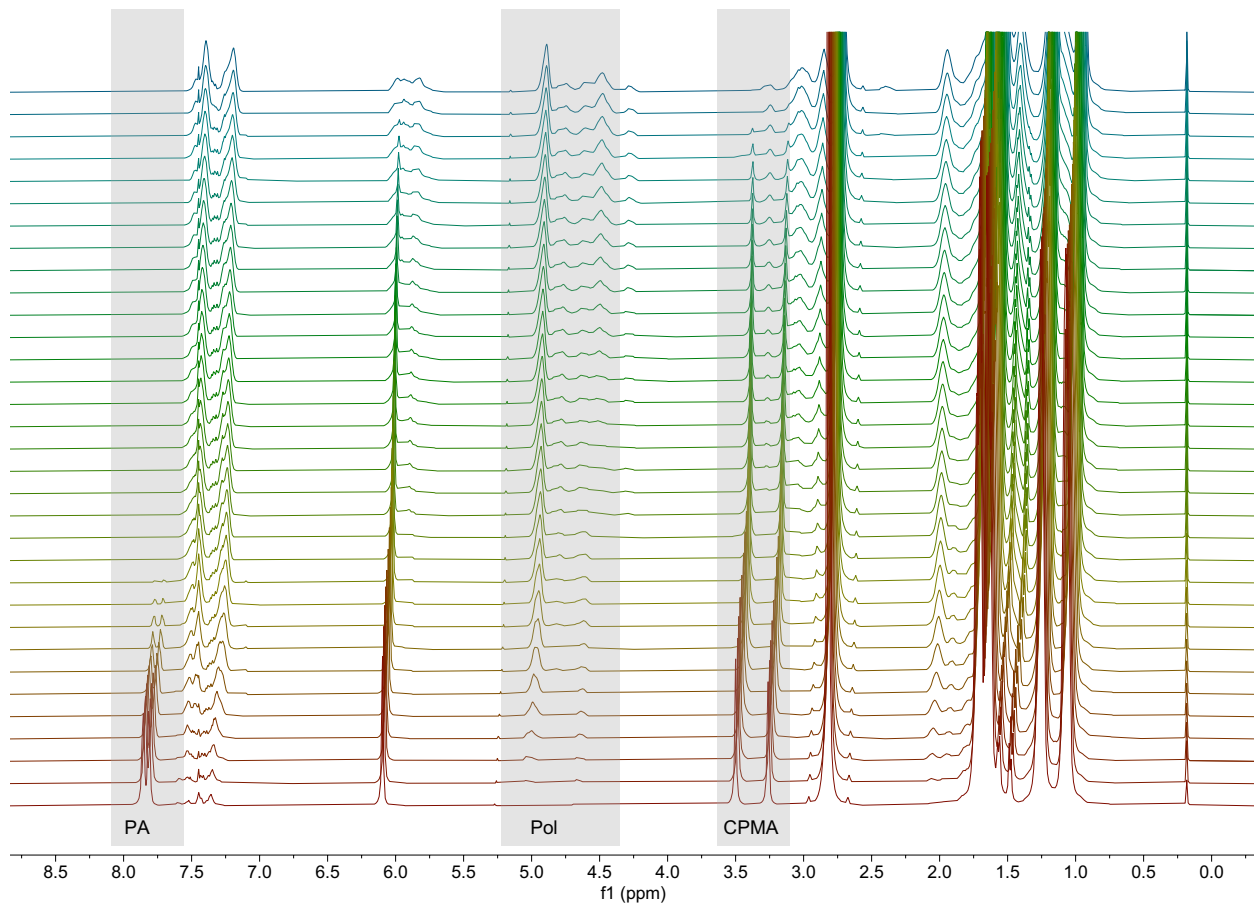


Fig. S13 ¹H NMR spectra of CHO/PA-*b*-CHO/CPMA monitored at 110 °C (Fig. 3b).

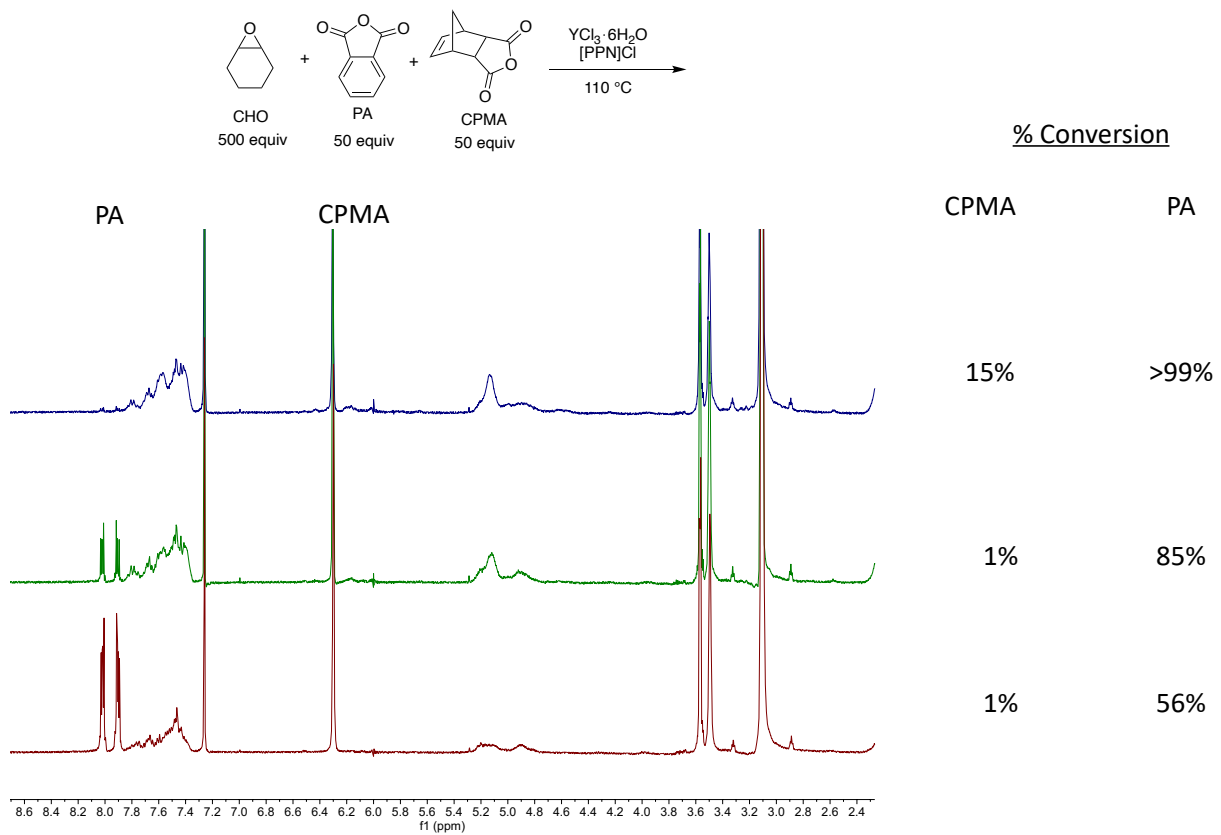


Fig. S14 ^1H NMR spectra of CHO/PA-*b*-CHO/CPMA in CDCl_3 monitored by aliquots.

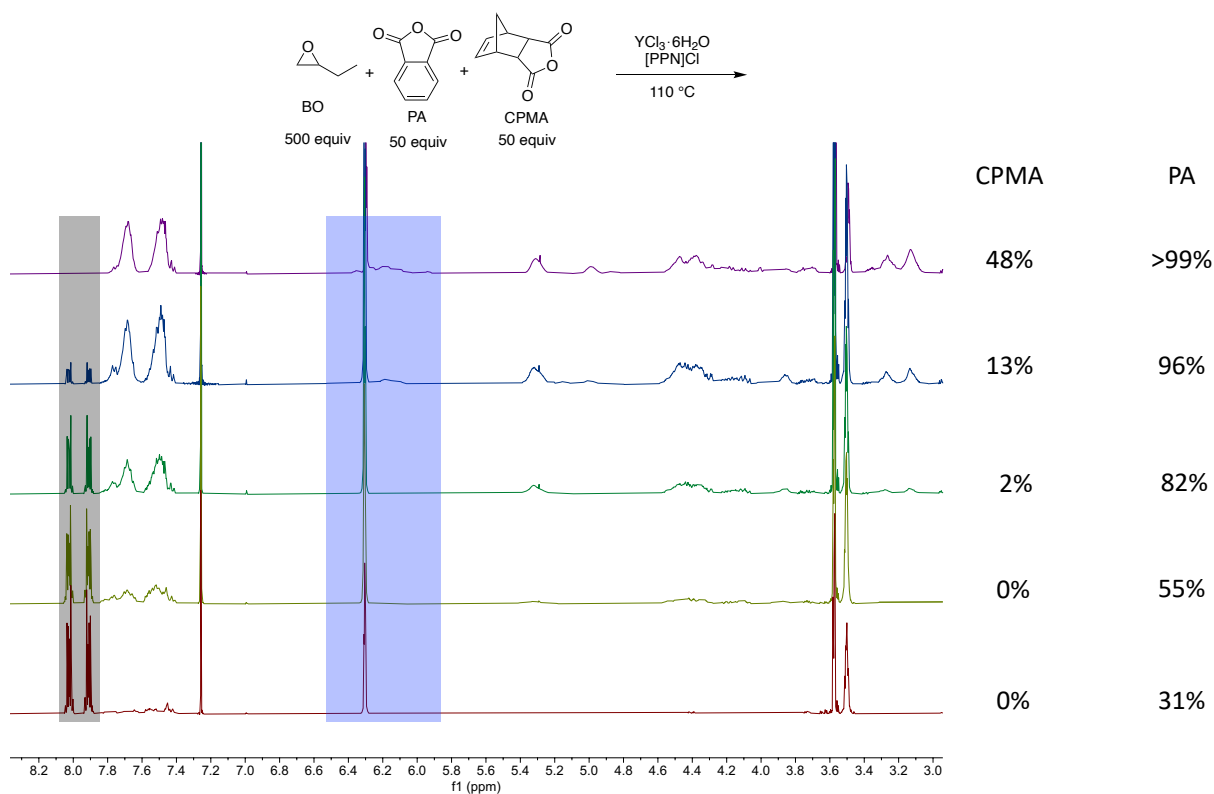


Fig. S15 ^1H NMR spectra of BO/PA-*b*-BO/CPMA in CDCl_3 monitored by aliquots.

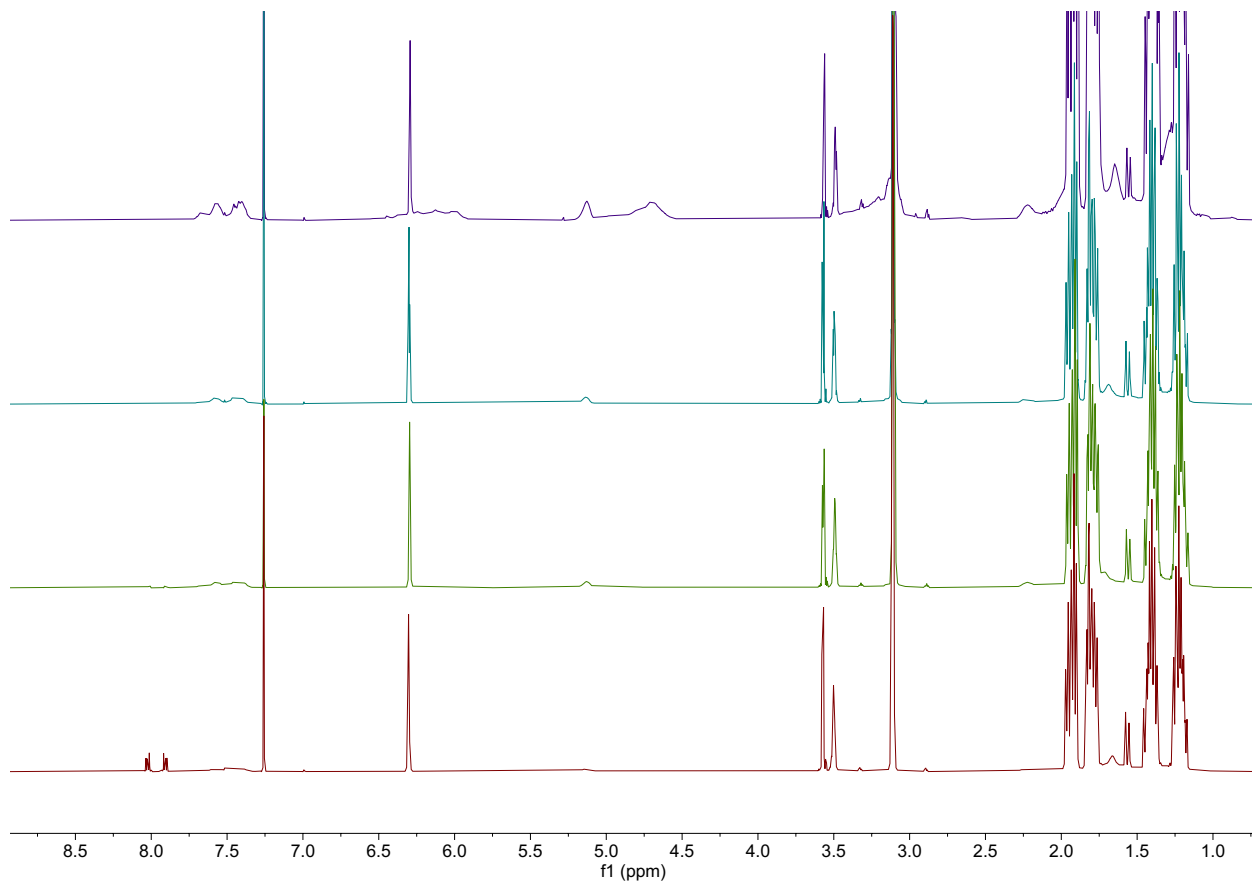


Fig. S16 ¹H NMR spectra of aliquots for CHO/PA-*b*-CHO/CPMA in CDCl₃ (Table S4, Entry 1). Aliquots taken at 30 min, 1 hr, 1.5 hr, and 4 hr.

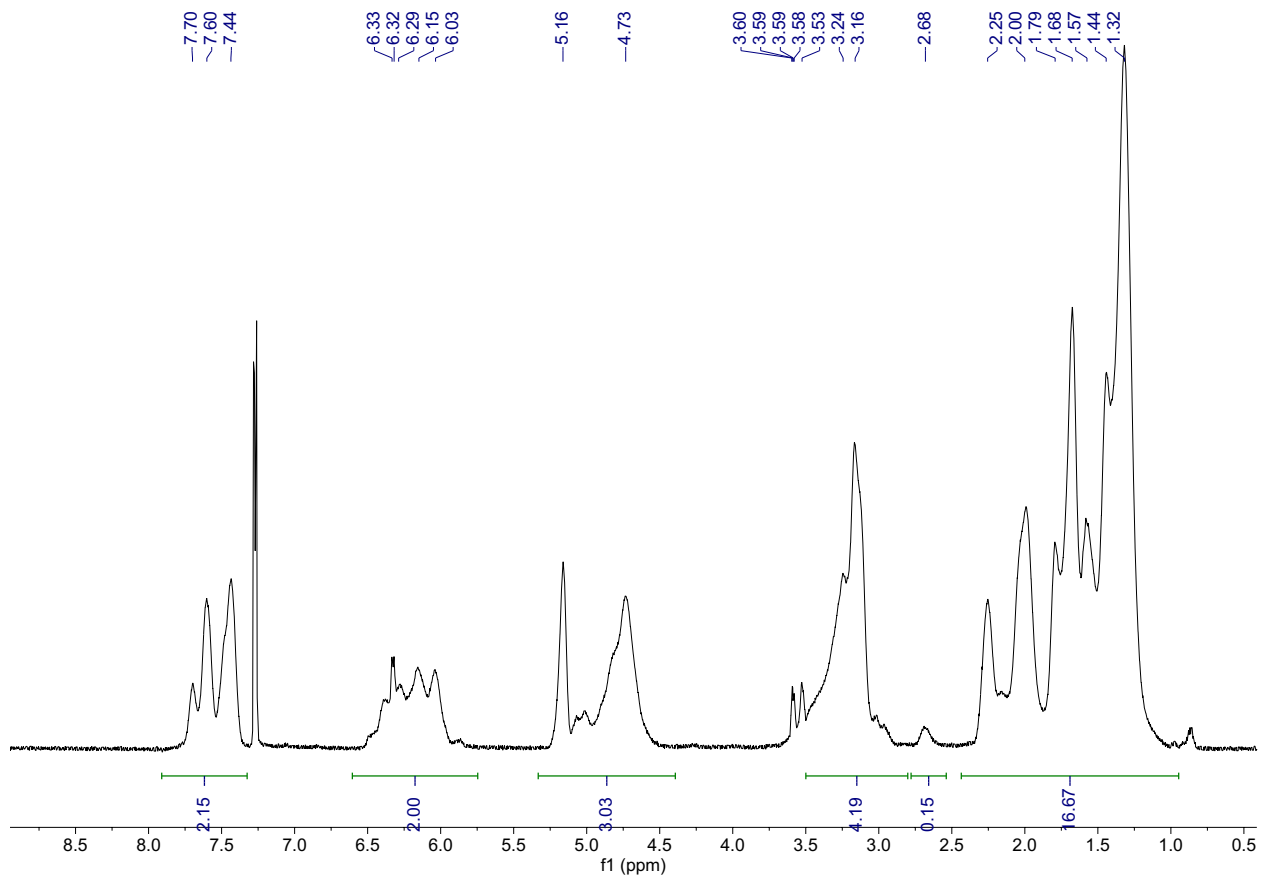


Fig. S17 ${}^1\text{H}$ NMR of CHO/PA-*b*-CHO/CPMA in CDCl_3 (Table S4, Entry 1)

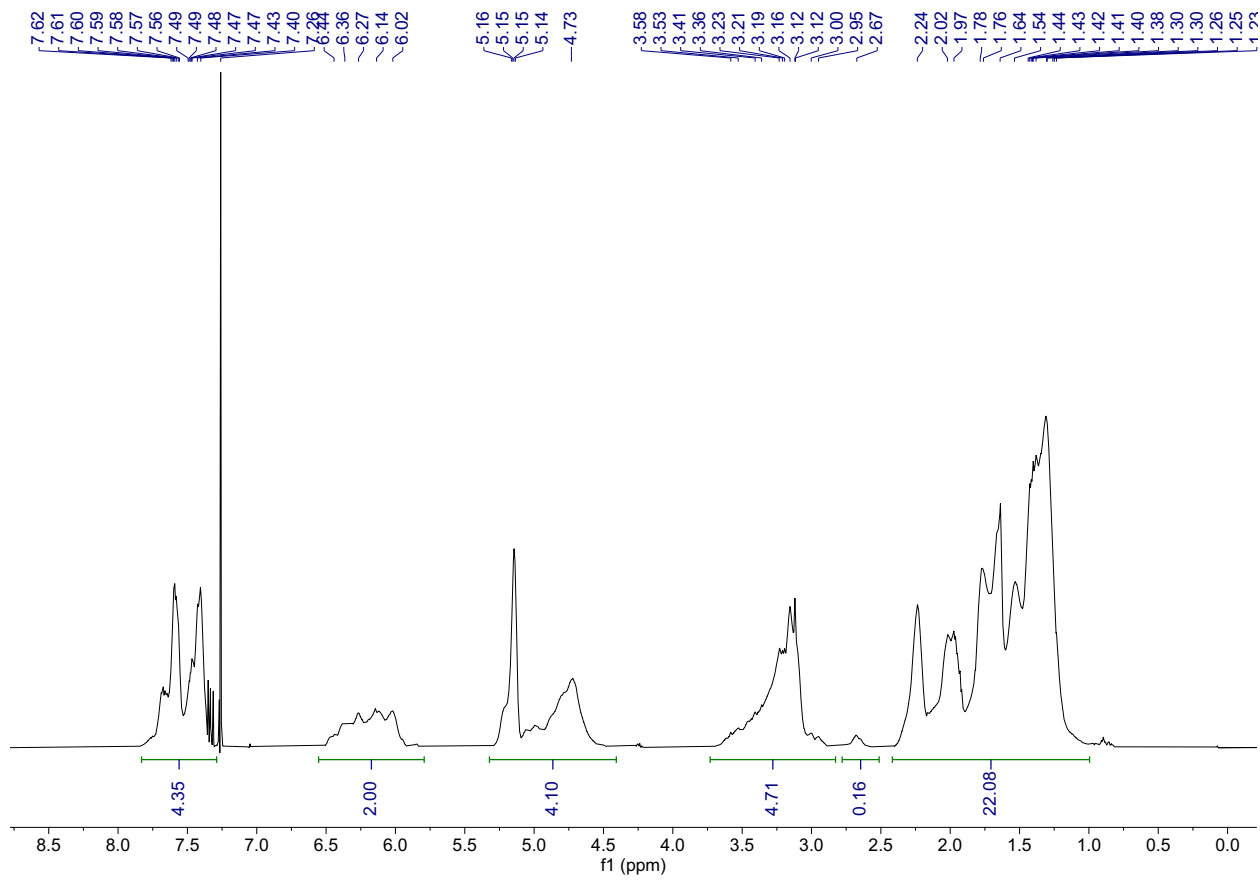


Fig. S18 ^1H NMR of CHO/PA-*b*-CHO/CPMA in CDCl_3 (Table S4, Entry 2).

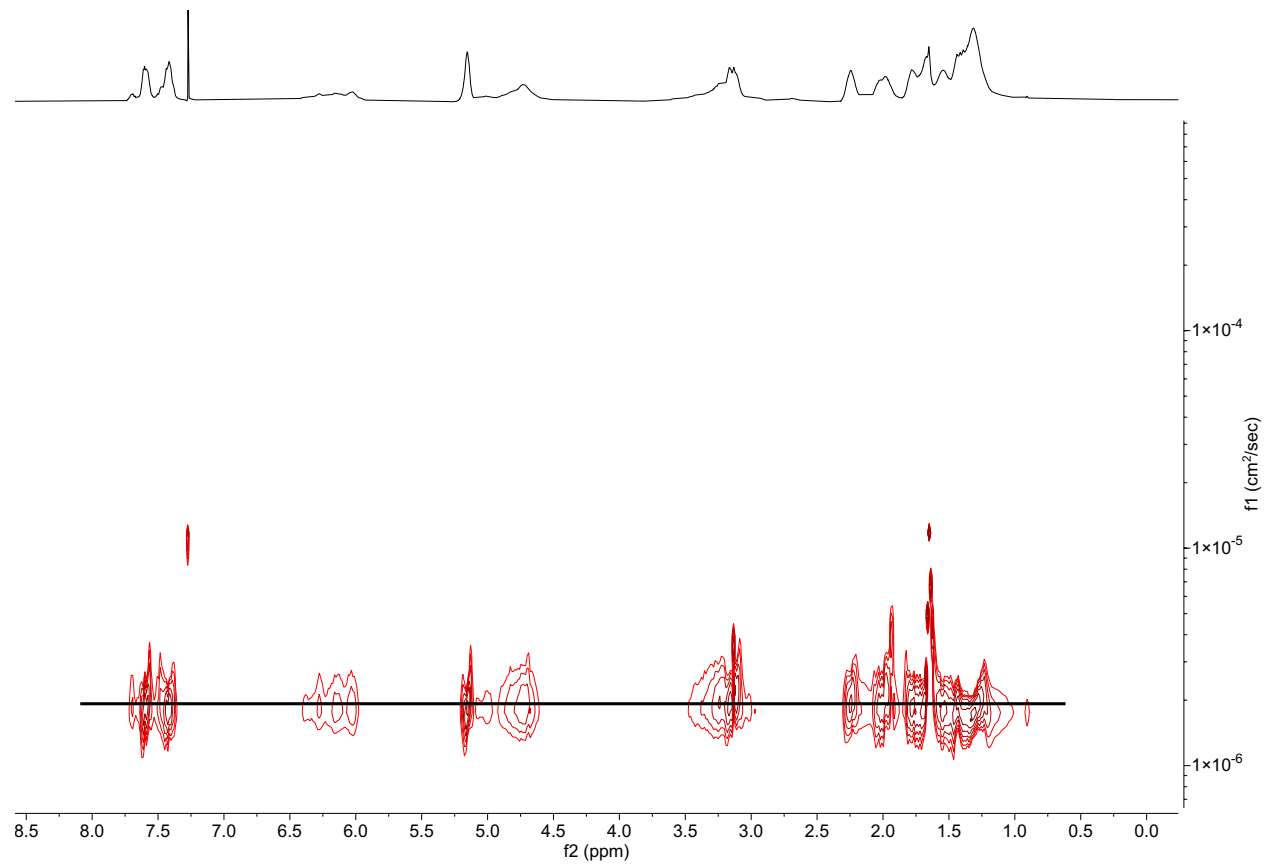


Fig. S19 ¹H DOSY of CHO/PA-*b*-CHO/CPMA in CDCl₃ (Table S4, Entry 2).

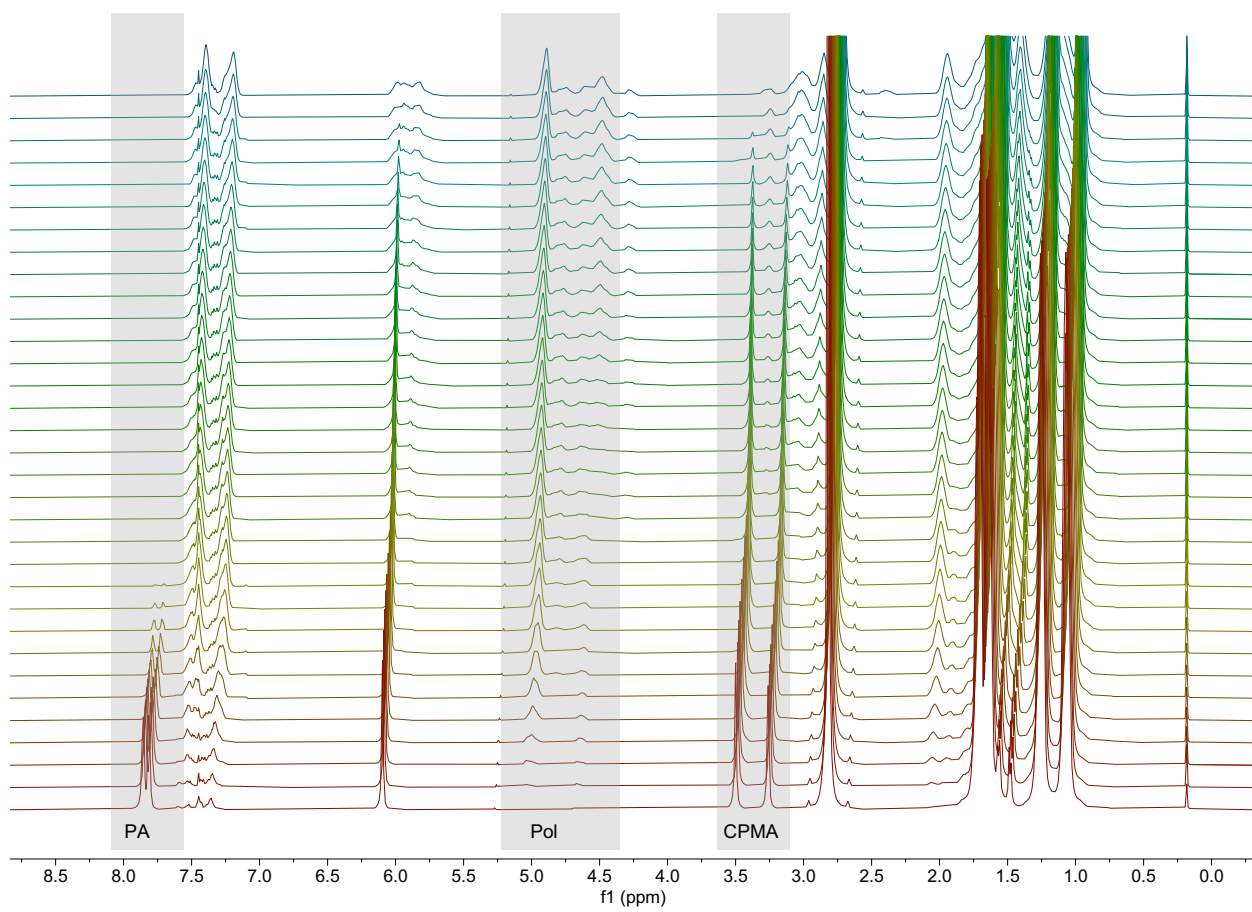


Fig. S20 ¹H NMR spectra of CHO/GA-*r*-CHO/CPMA monitored at 110 °C (Fig. 3c).

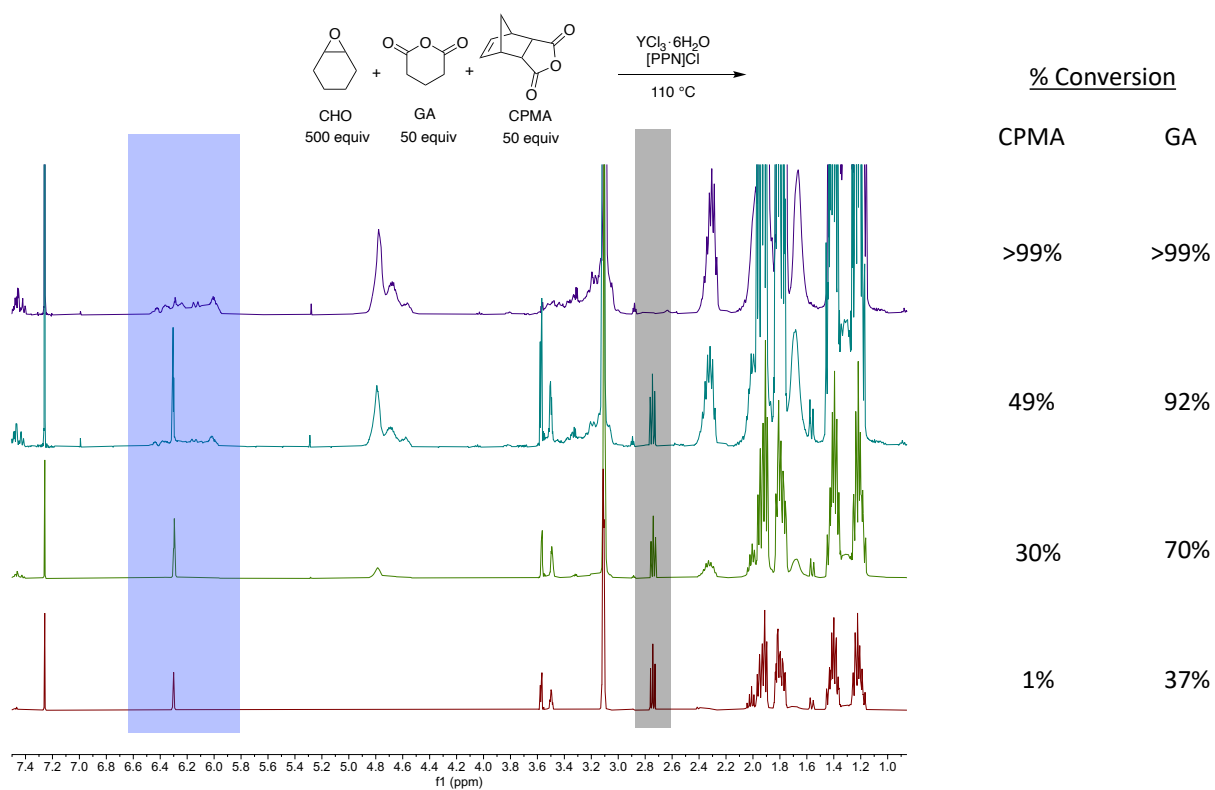


Fig. S21 ^1H NMR spectra of CHO/GA-*r*-CHO/CPMA in CDCl_3 monitored by aliquots.

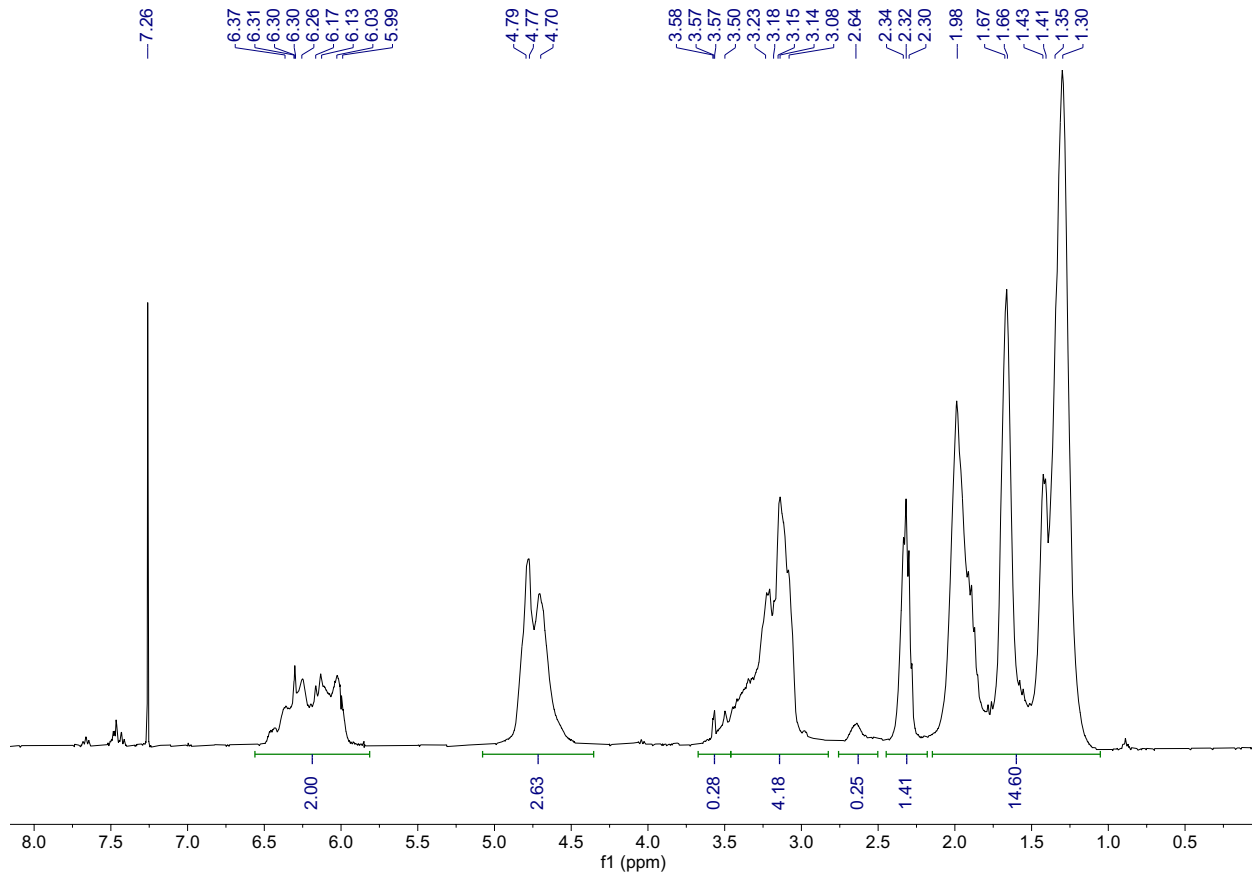


Fig. S22 ${}^1\text{H}$ NMR spectrum of CHO/GA-*r*-CHO/CPMA in CDCl_3 (Table S4, Entry 3).

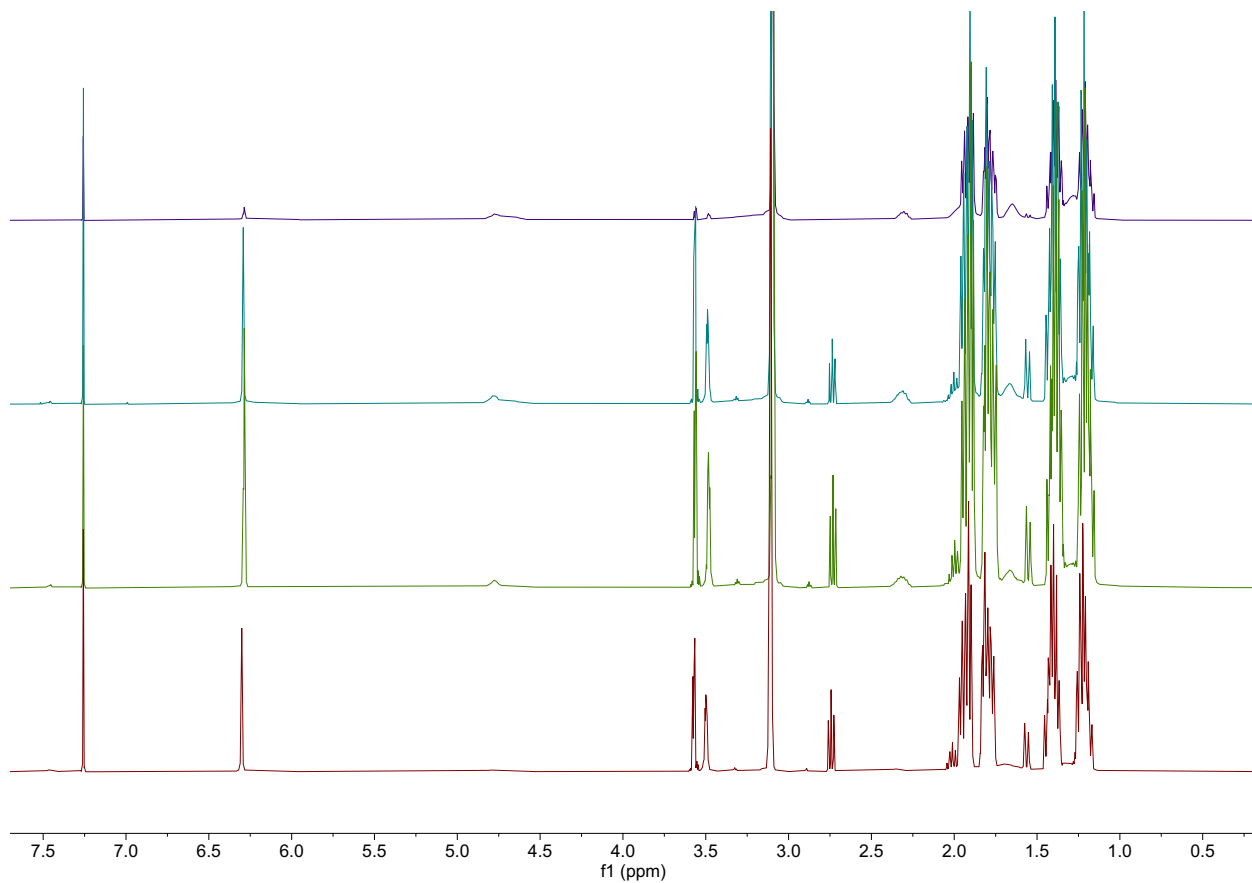


Fig. S23 ^1H NMR spectra stack of CHO/GA-*r*-CHO/CPMA in CDCl_3 (Table S4, Entry 3). Aliquots taken at 30 min, 1 hr, 1.5 hr, and 4 hr (from bottom to top).

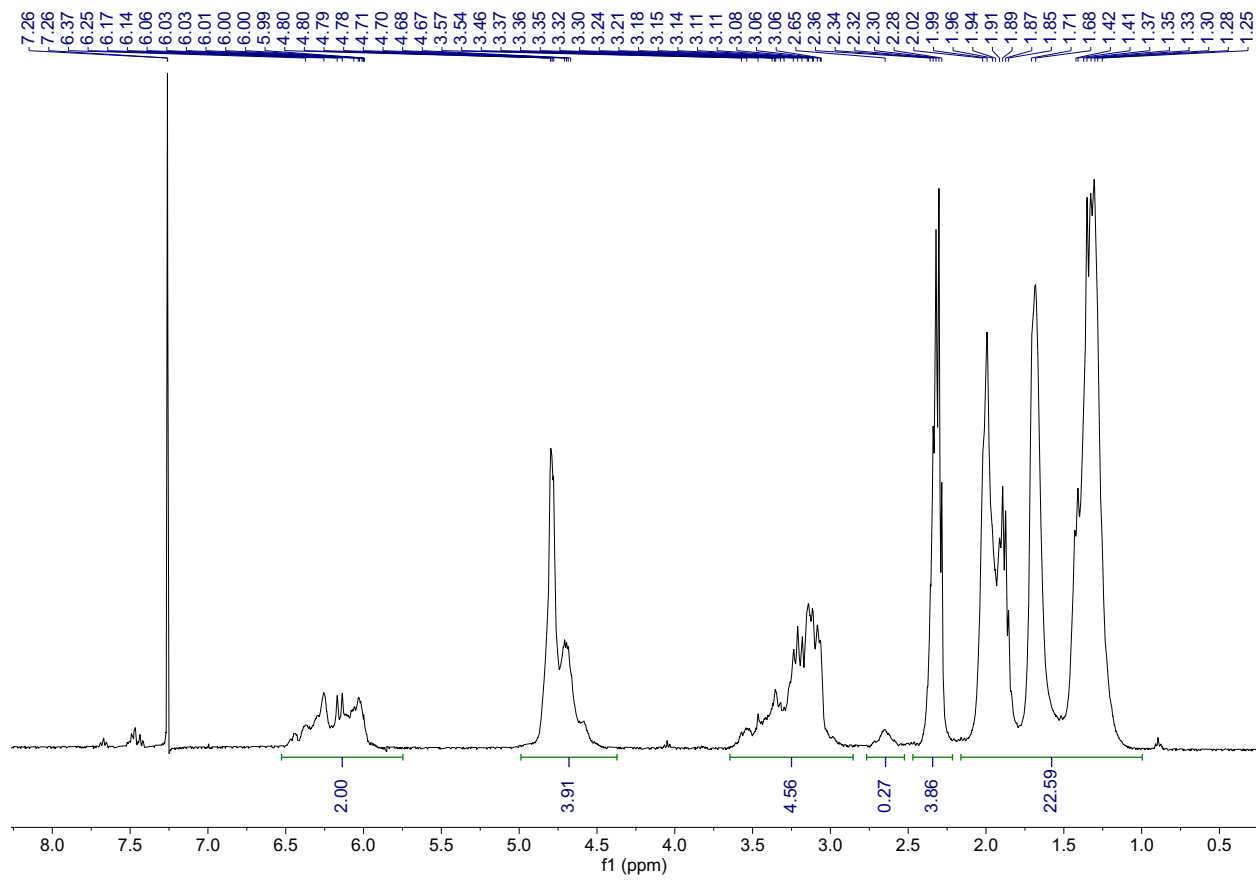


Fig. S24 ^1H NMR of CHO/GA-*r*-CHO/CPMA in CDCl_3 (Table S4, Entry 4).

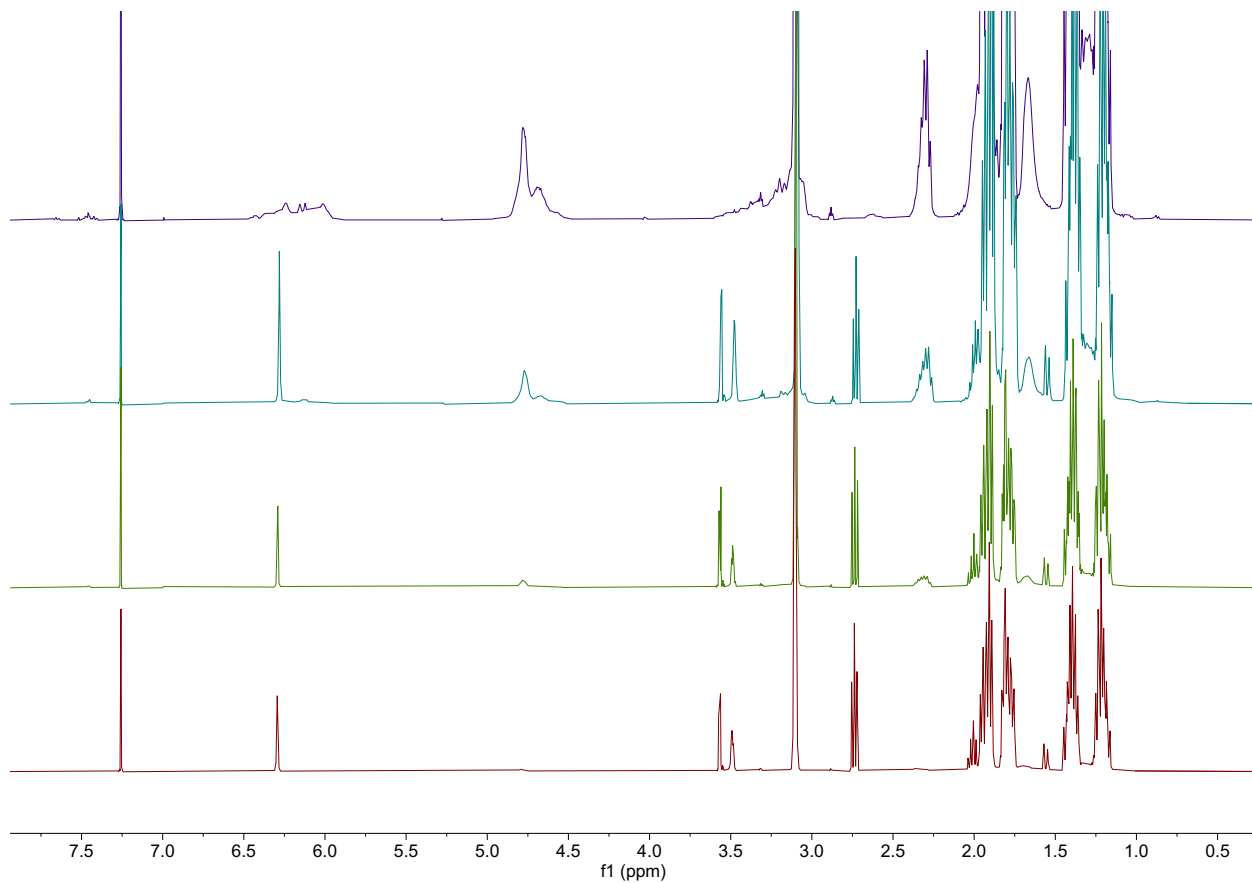


Fig. S25 ¹H NMR spectra stack of CHO/GA-*r*-CHO/CPMA in CDCl₃ (Table S4, Entry 4). Aliquots taken at 30 min, 1 hr, 1.5 hr, and 4 hr (from bottom to top).

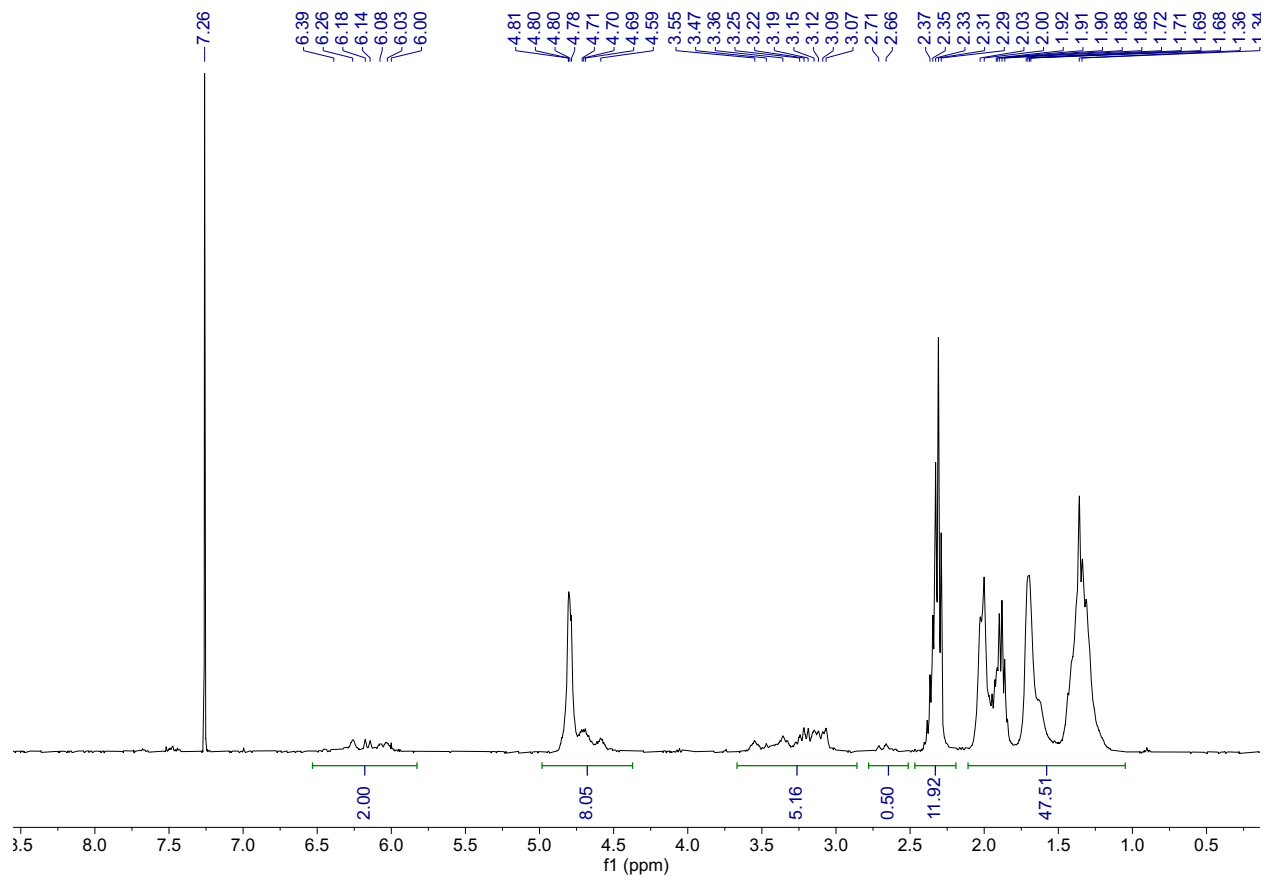


Fig. S26 ^1H NMR of CHO/GA-*r*-CHO/CPMA in CDCl_3 (Table S4, Entry 5).

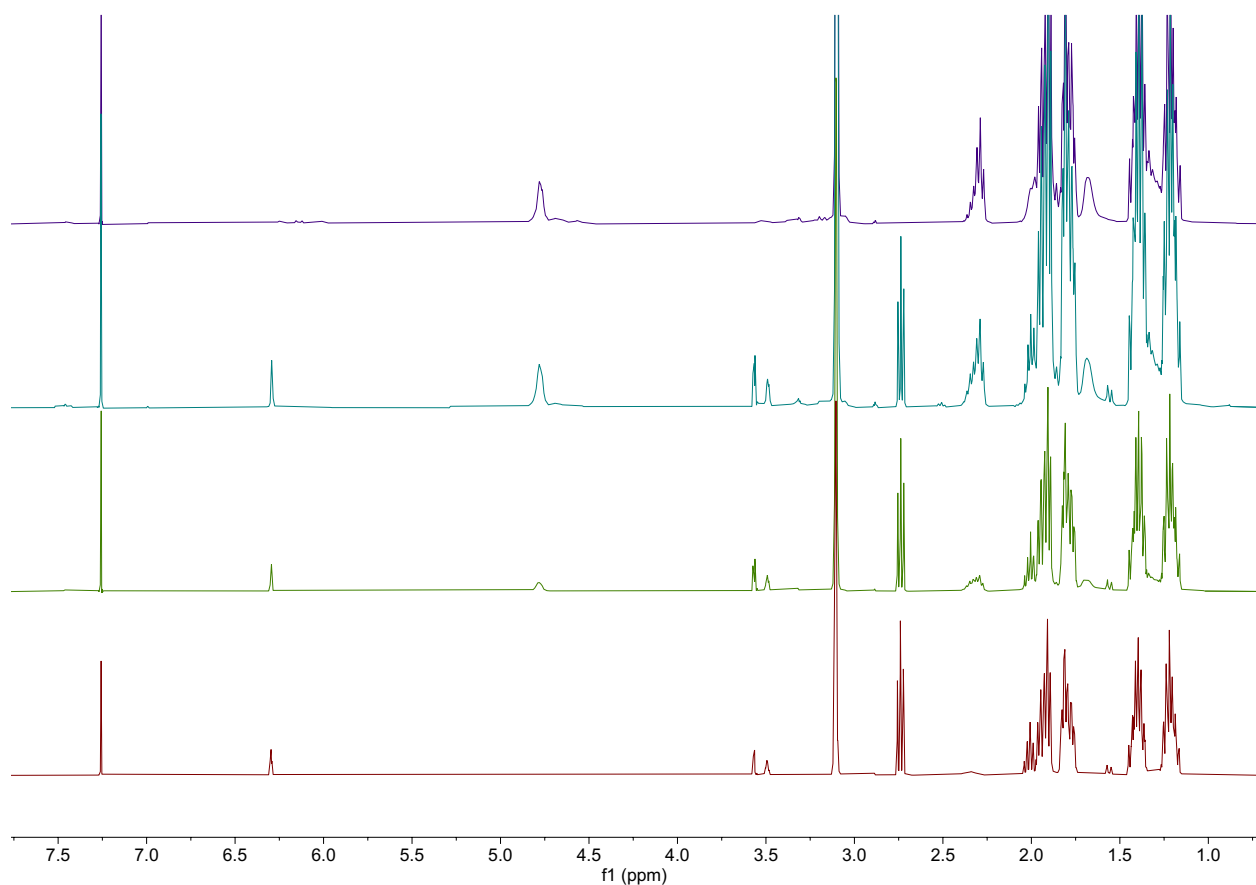


Fig. S27 ¹H NMR spectra stack of CHO/GA-*r*-CHO/CPMA in CDCl₃ (Table S4, Entry 5). Aliquots taken at 30 min, 1 hr, 1.5 hr, and 4 hr (from bottom to top).

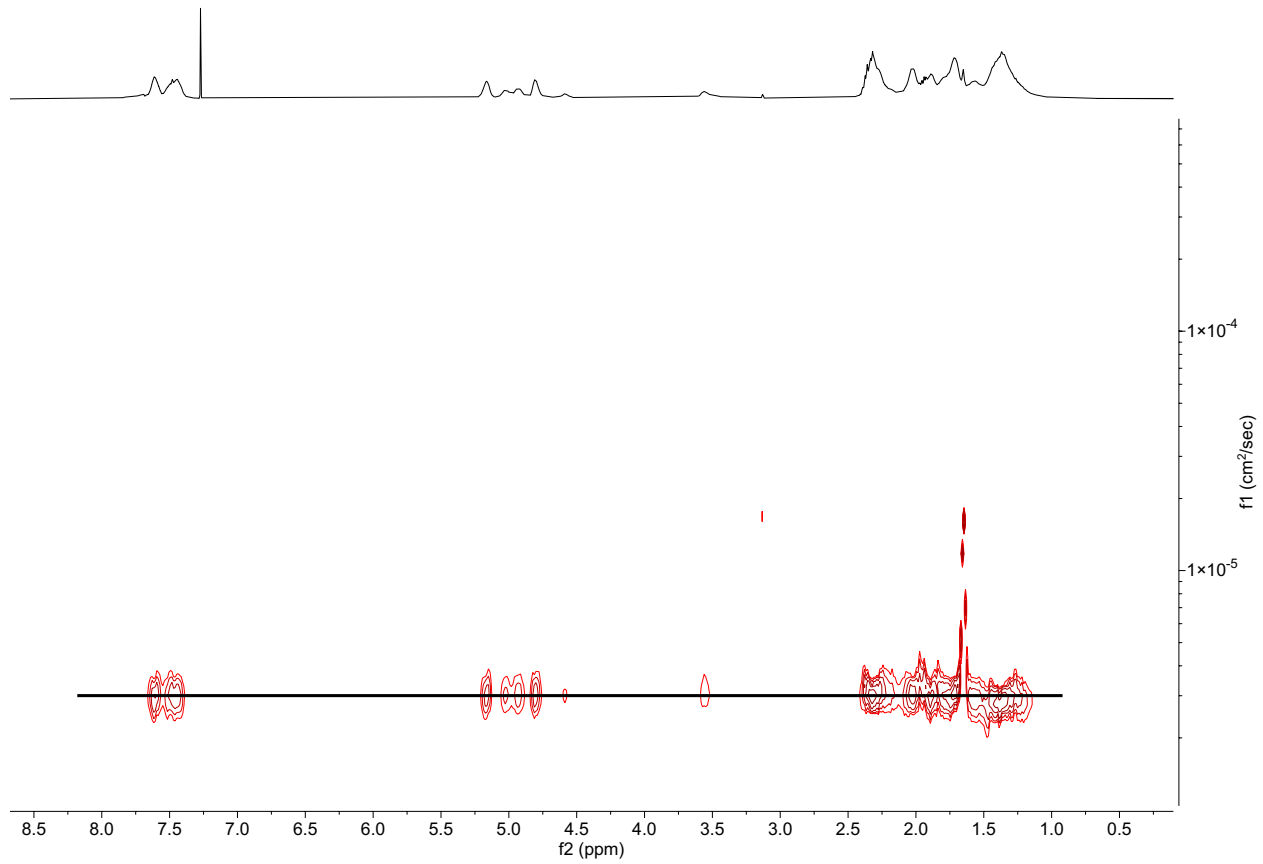


Fig. S28 ^1H DOSY of CHO/GA-*r*-CHO/CPMA in CDCl_3 (Table S4, Entry 5).

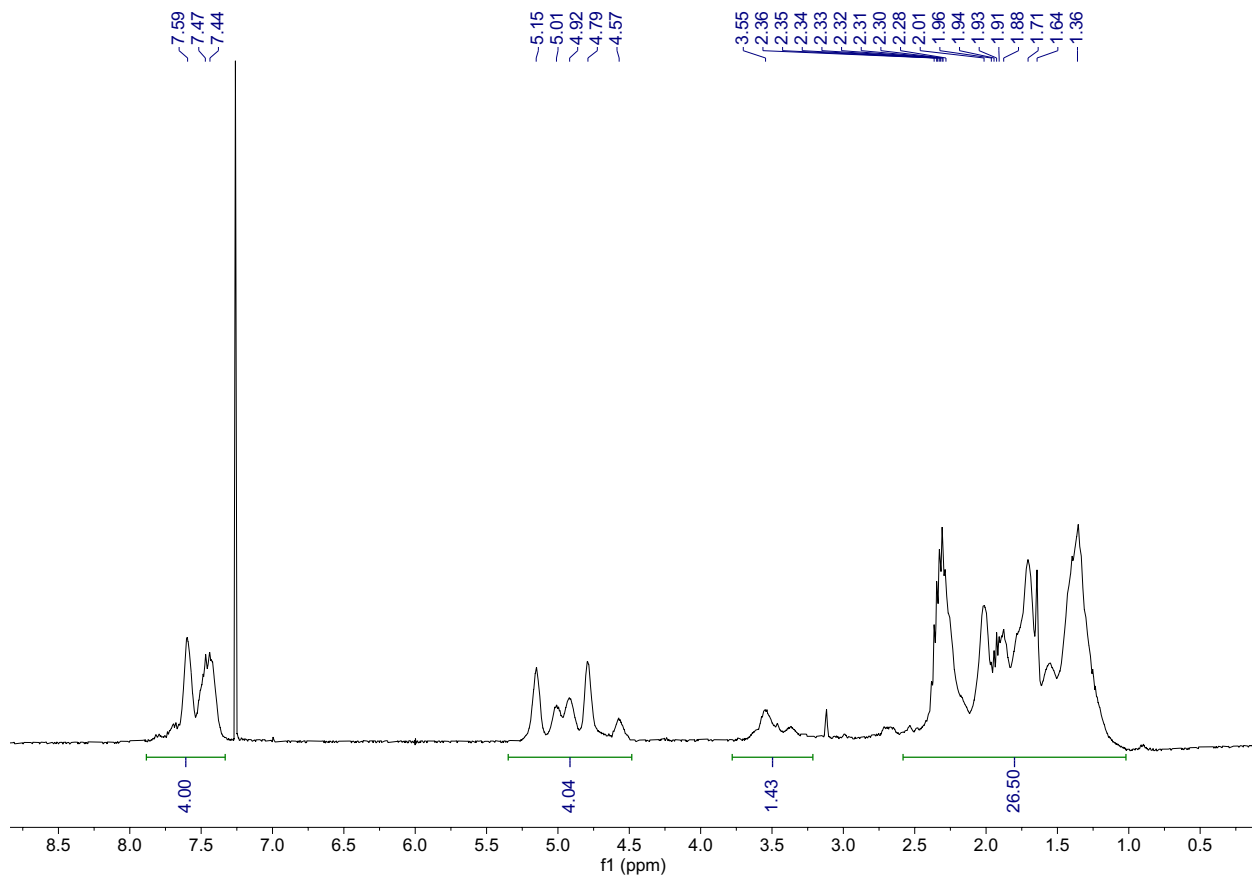


Fig. S29 ^1H NMR of CHO/PA-*r*-CHO/GA in CDCl_3 (Table S4, Entry 6).

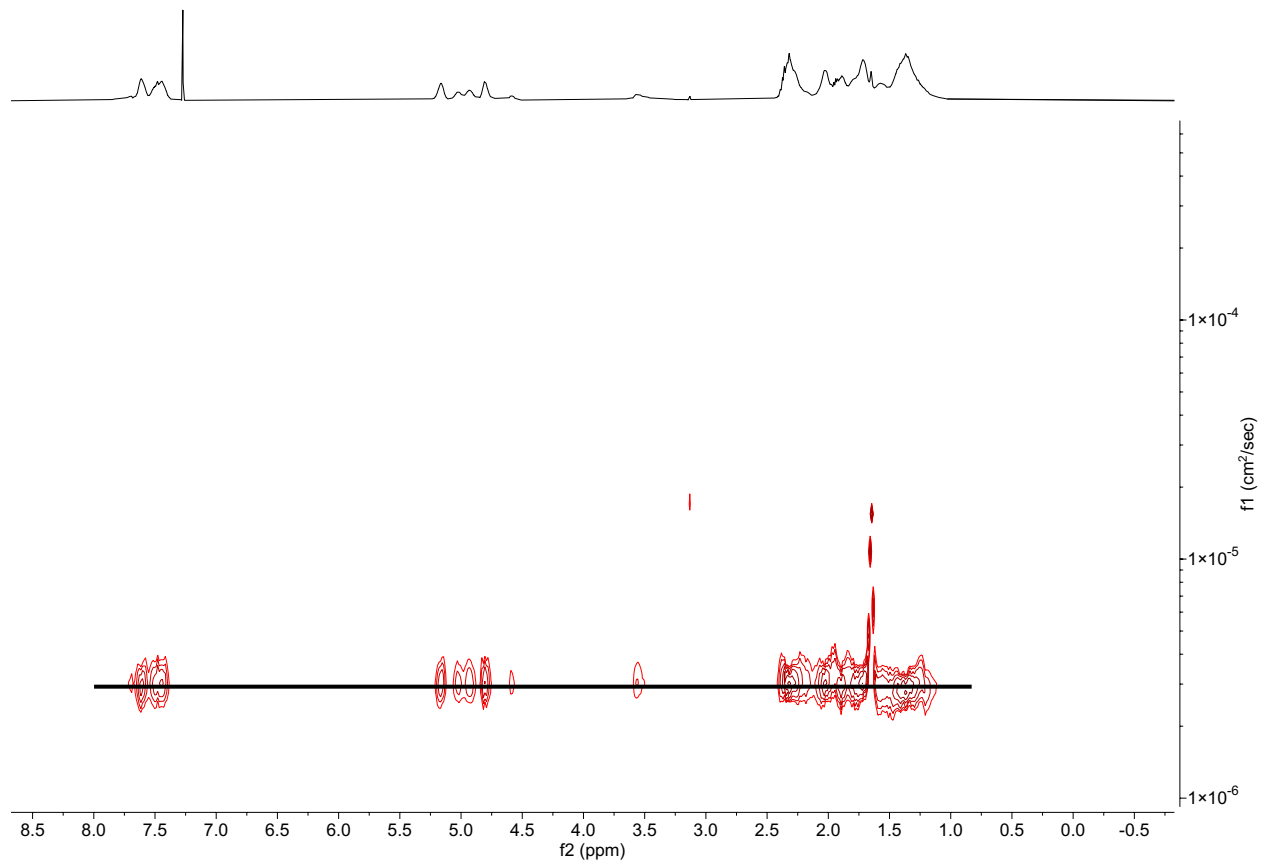


Fig. S30 ^1H DOSY of CHO/PA-*r*-CHO/GA in CDCl_3 (Table S4, Entry 6).

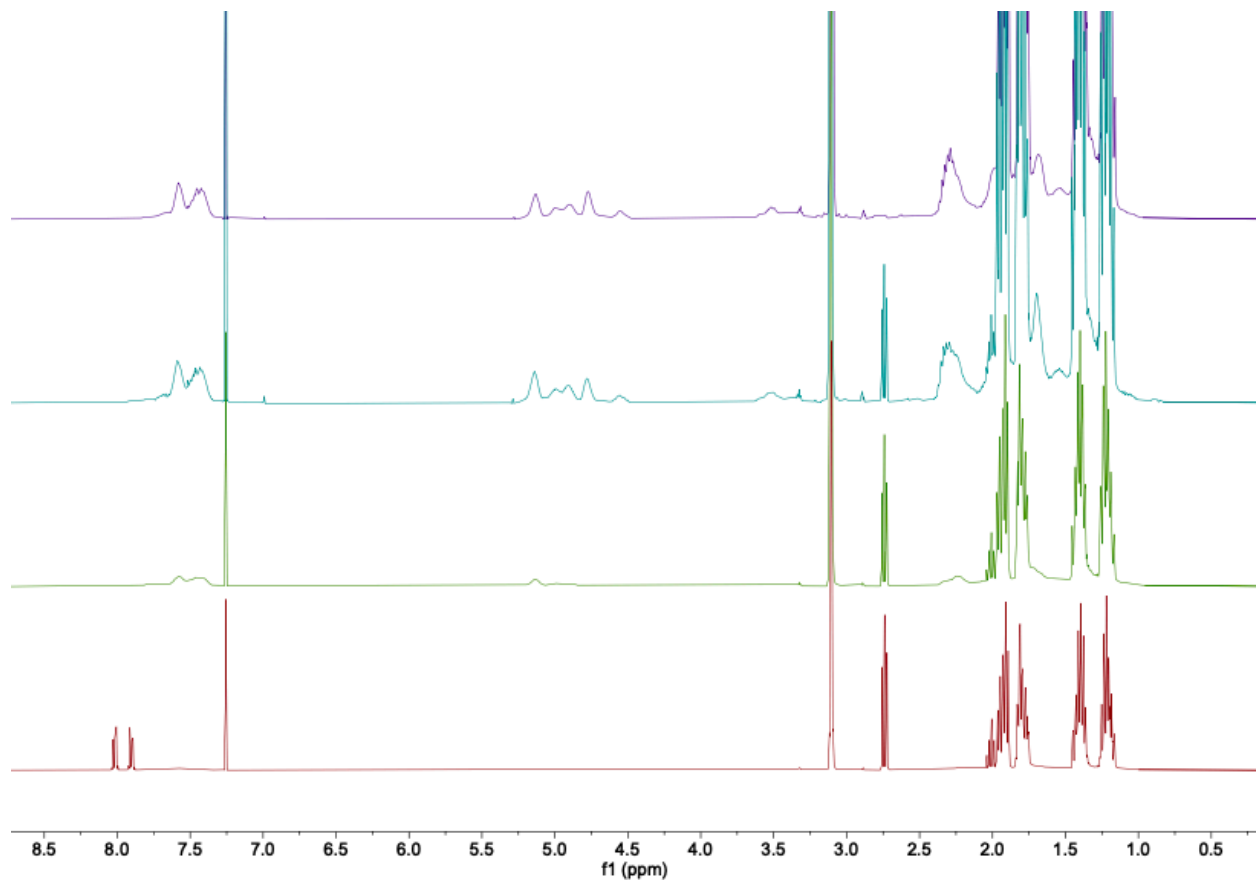


Fig. S31 ¹H NMR spectra stack of CHO/GA-*r*-CHO/CPMA in CDCl₃ (Table S4, Entry 6). Aliquots taken at 30 min, 1 hr, 1.5 hr, and 4 hr (from bottom to top).

5.2 Anhydride ring-opening studies. To get reactivity ratios between anhydride mixtures, we adopted a procedure from Satoh and coworkers that involves the use of an alcohol and observing the ring opened anhydride products by ^1H NMR.⁴

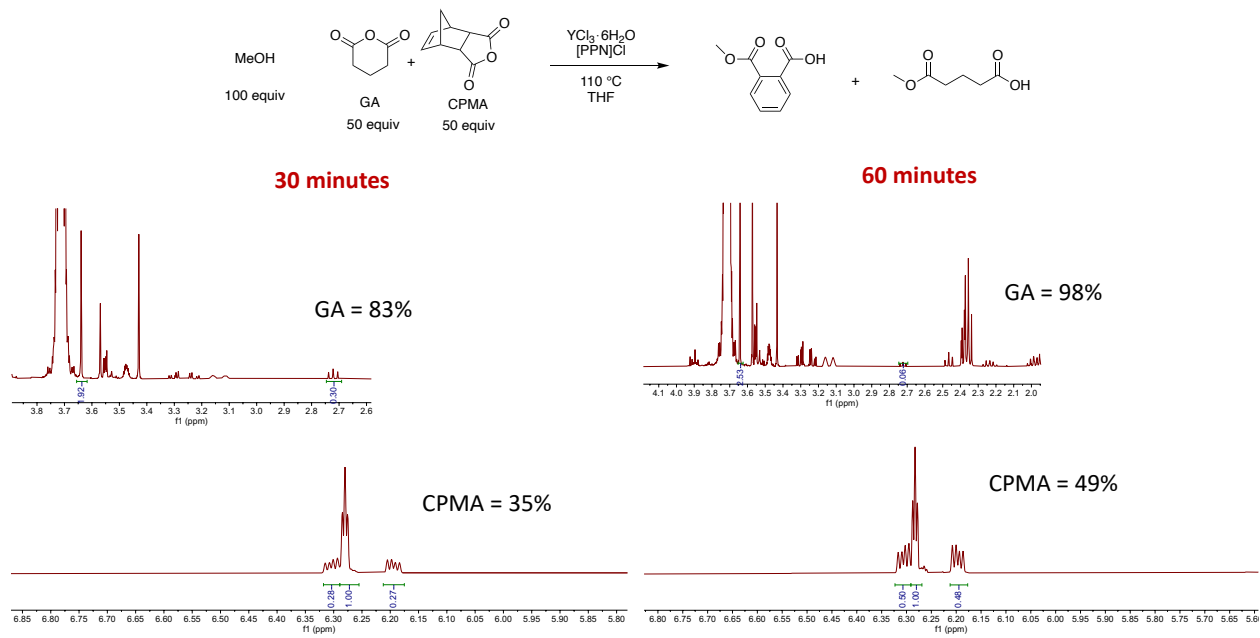


Fig. S32 ^1H NMR analysis of aliquots from the reaction of GA and CPMA with 100 equivalents of MeOH, catalyzed by $\text{YCl}_3 \cdot 6\text{H}_2\text{O}/[\text{PPN}]\text{Cl}$. Reaction was performed in THF and heated at 110 °C. Aliquots taken at 30 minutes and 60 minutes.

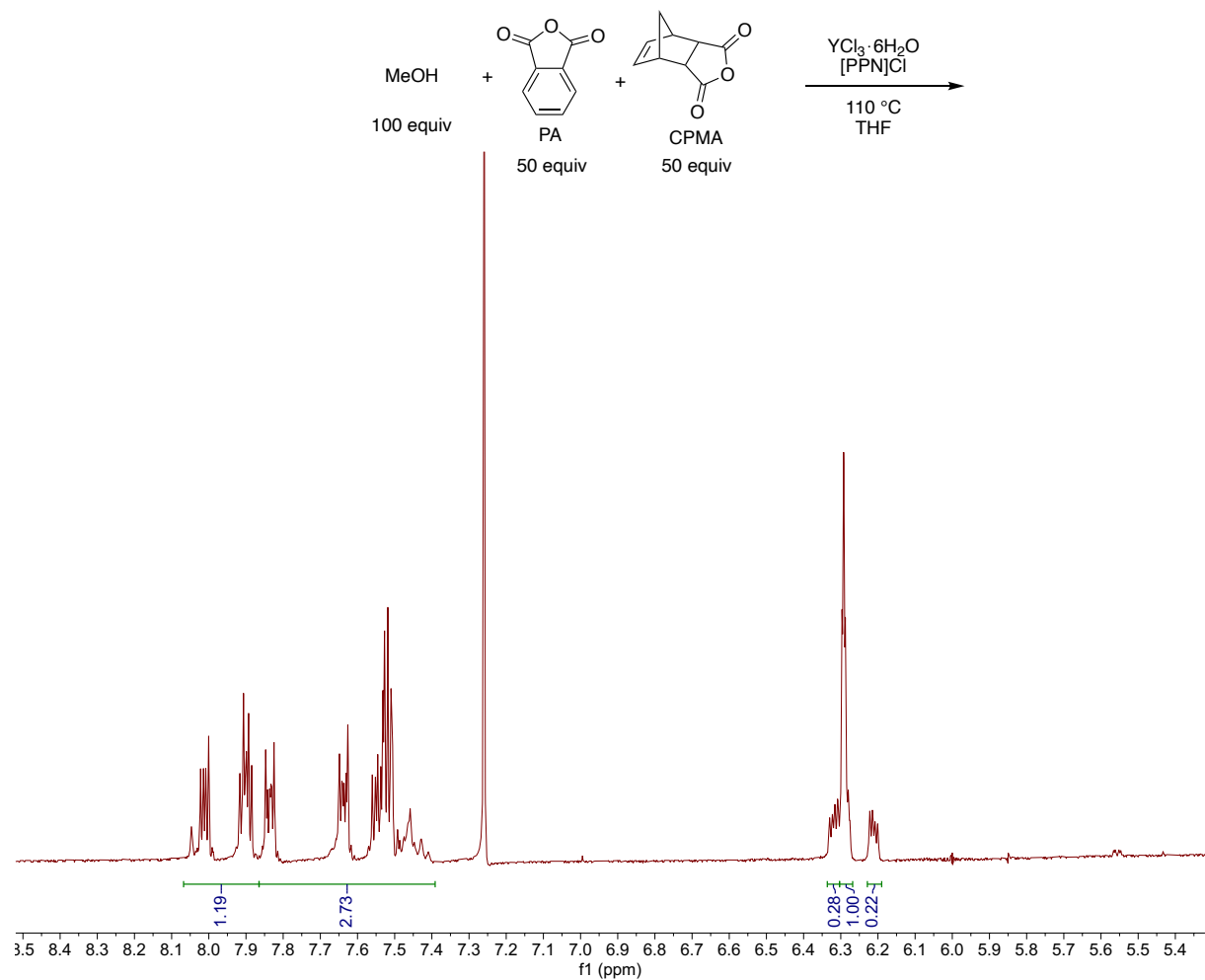


Fig. S33 ¹H NMR analysis of aliquots from the reaction of PA and CPMA with 100 equivalents of MeOH, catalyzed by YCl₃·6H₂O/[PPN]Cl. Reaction was performed in THF and heated at 110 °C. Aliquot taken at 1 hr. Ring-opening of CPMA occurs before ring-opening of PA is complete, conflicting with data from Fig. S60.

6. GPC Data

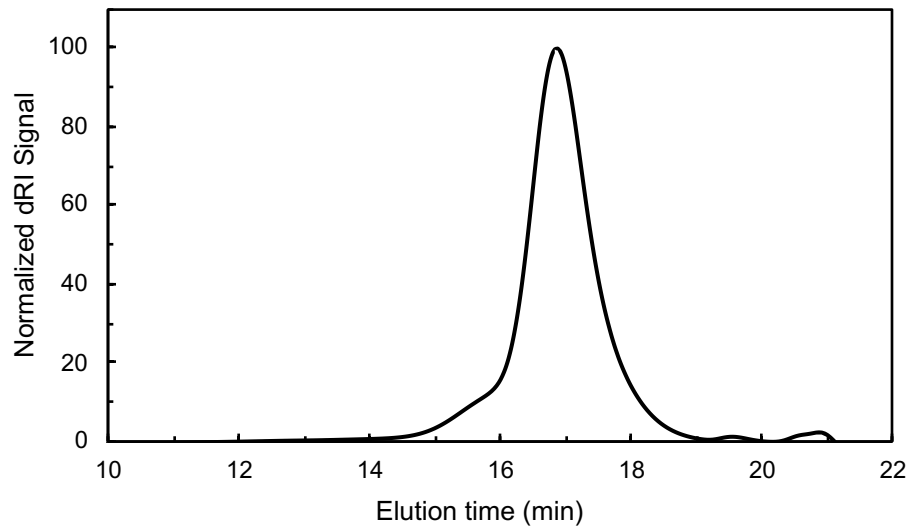


Fig. S34 GPC trace corresponding to Table 2, Entry 1.

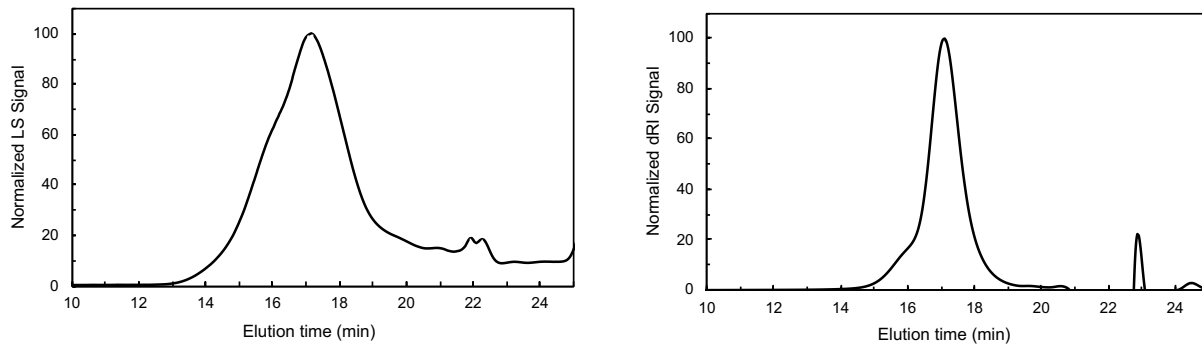


Fig. S35 GPC traces (MALS detector left, RI detector right) corresponding to Table 2, Entry 2.

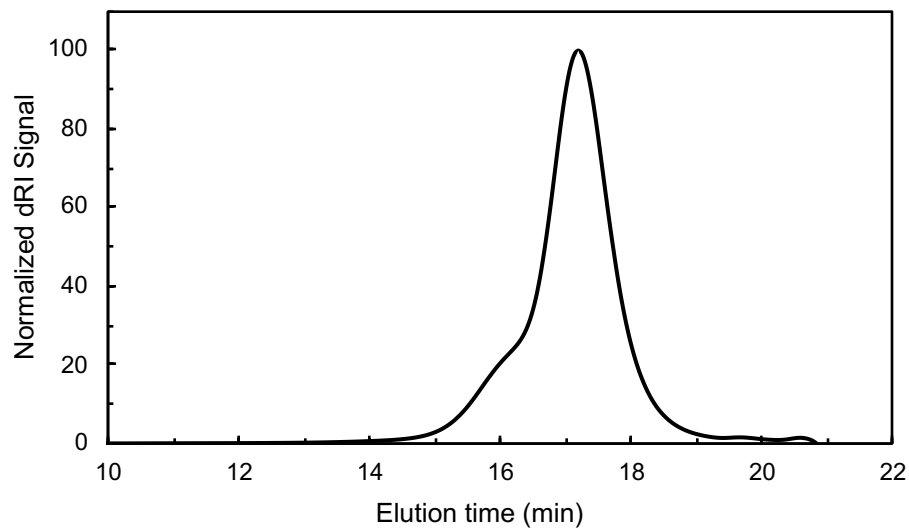


Fig. S36 GPC trace corresponding to Table 2, Entry 3.

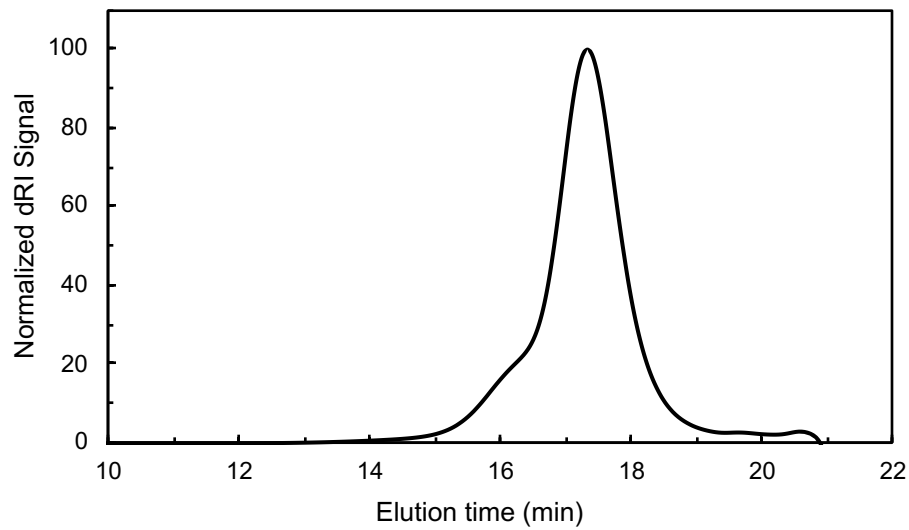


Fig. S37 GPC trace corresponding to Table 2, Entry 4.

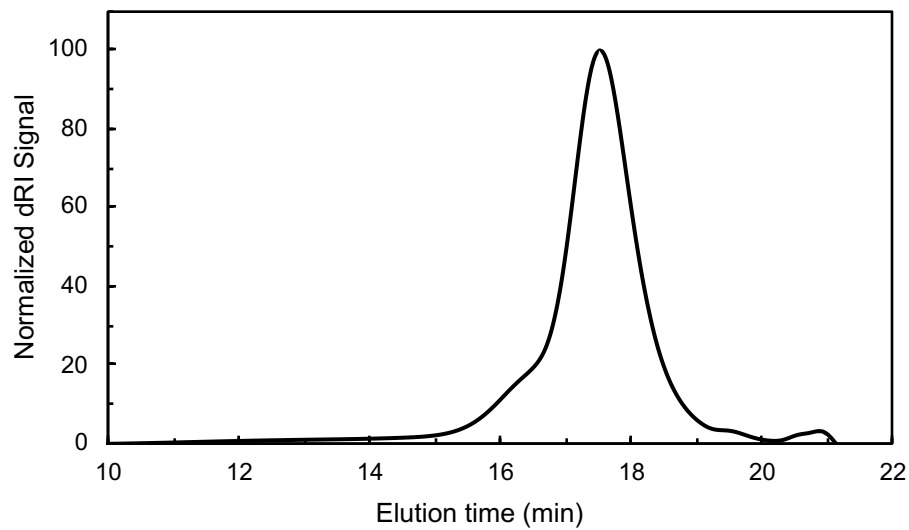


Fig. S38 GPC trace corresponding to Table 2, Entry 5.

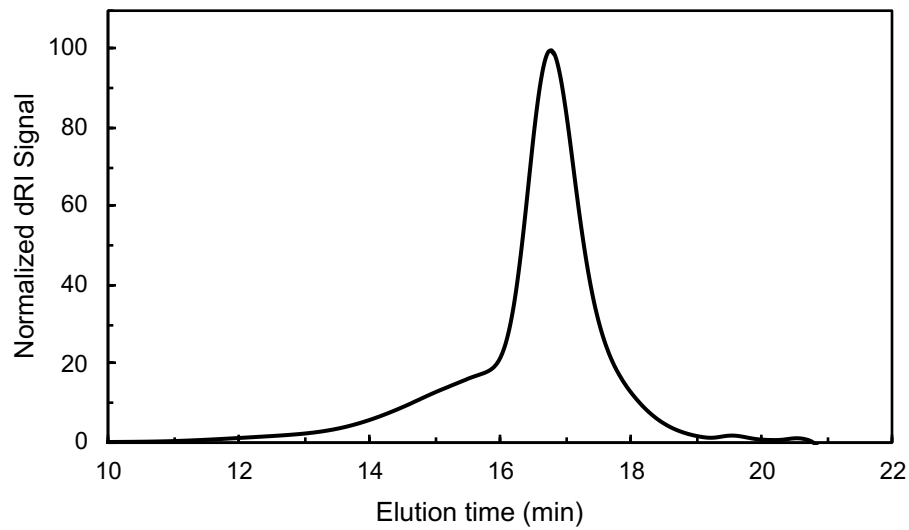


Fig. S39 GPC trace corresponding to Table S3, Entry 1.

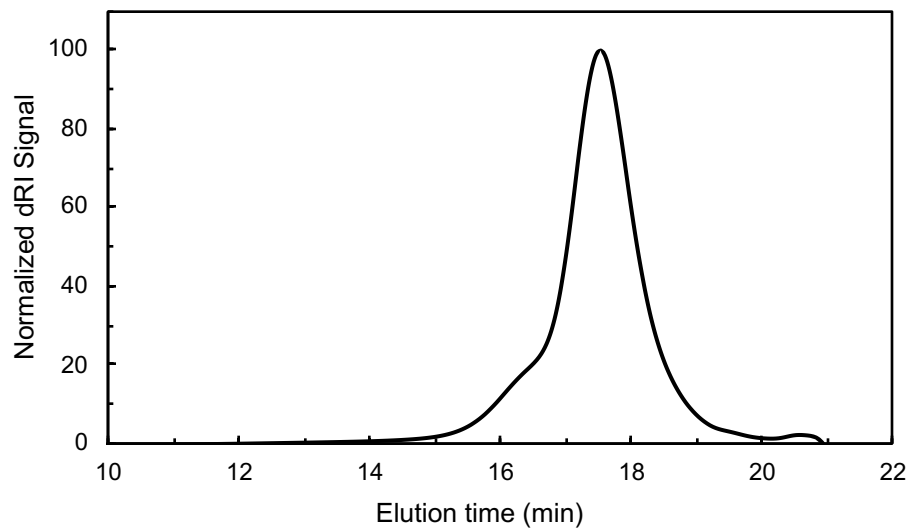


Fig. S40 GPC trace corresponding to Table S3, Entry 7.

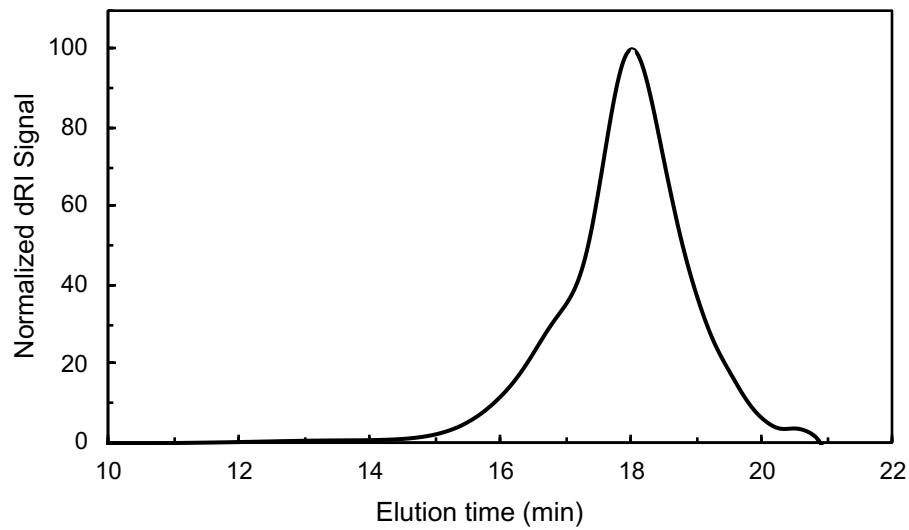


Fig. S41 GPC trace corresponding to Table S4, Entry 3.

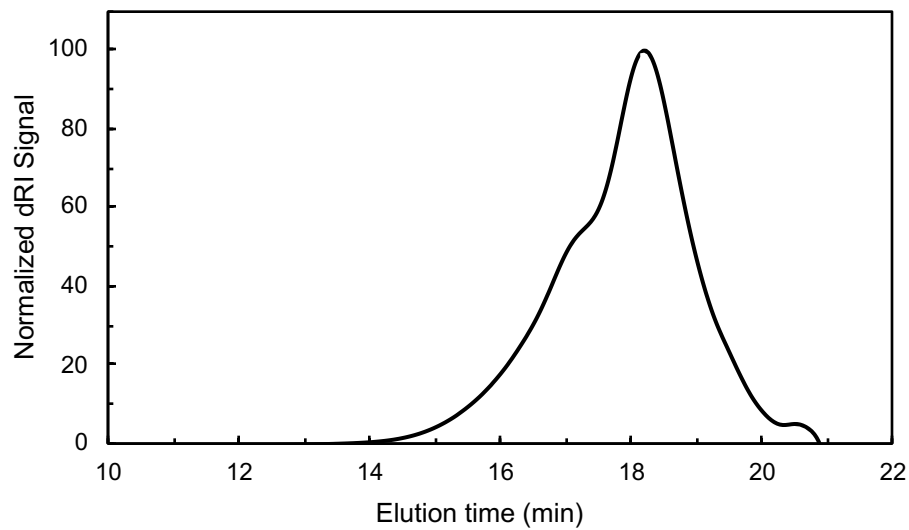


Fig. S42 GPC trace corresponding to Table S4, Entry 4.

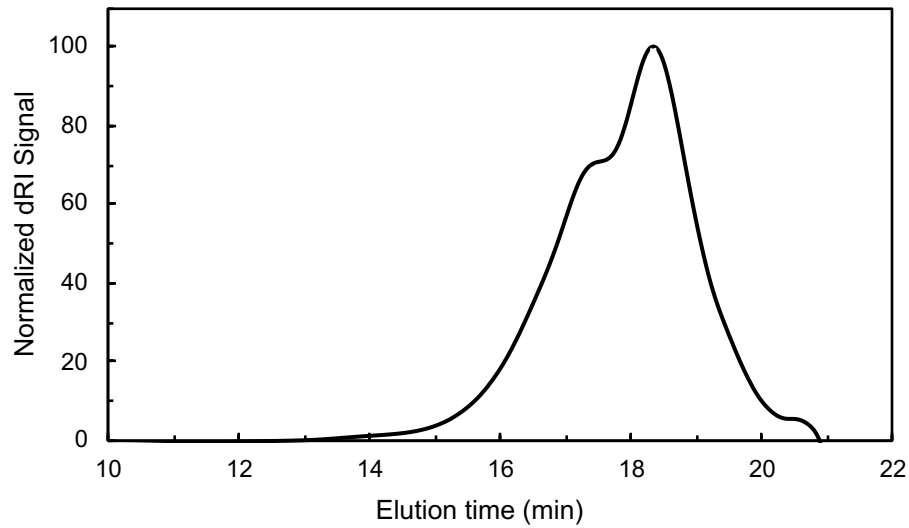


Fig. S43 GPC trace corresponding to Table S4, Entry 5.

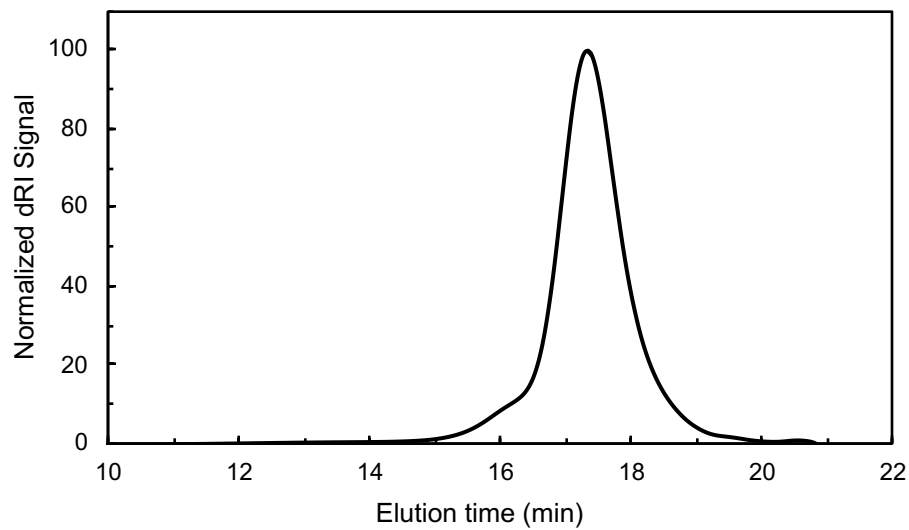


Fig. S44 GPC trace corresponding to Table S4, Entry 1.

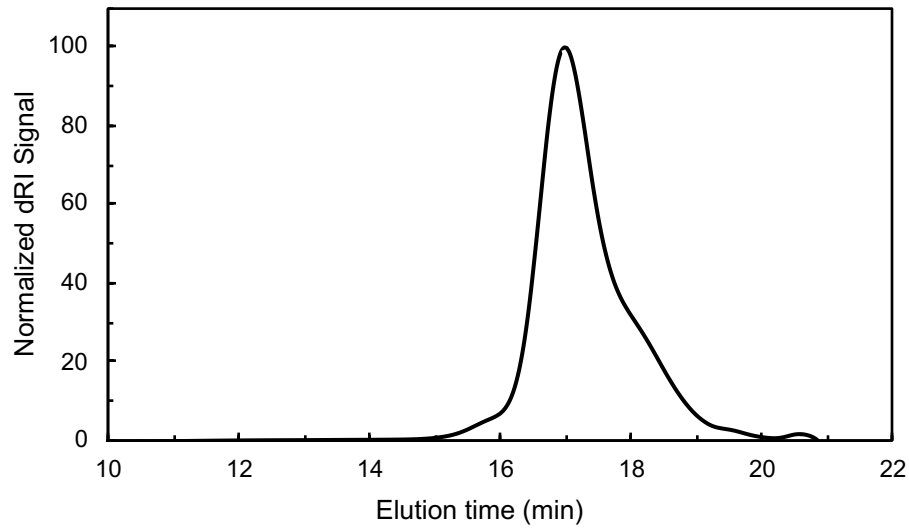


Fig. S45 GPC trace corresponding to Table S4, Entry 2.

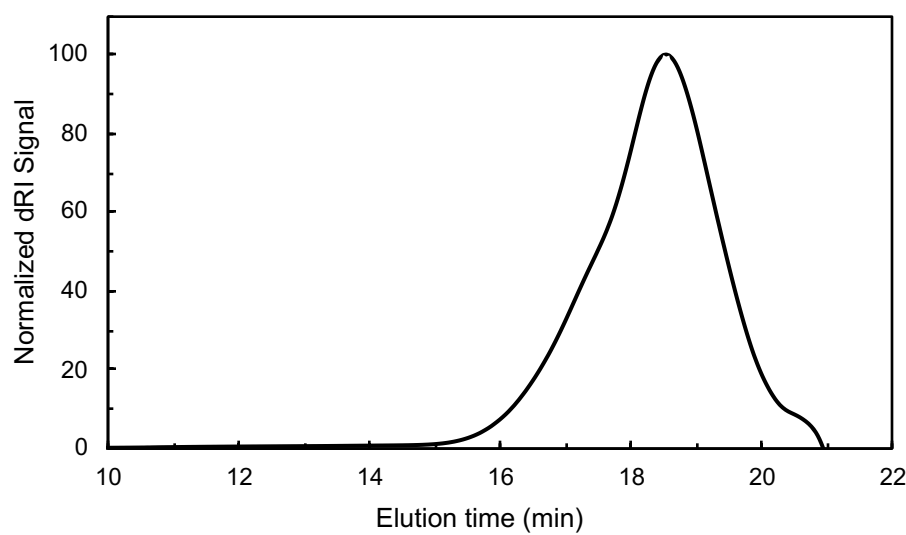


Fig. S46 GPC trace corresponding to Table S4, Entry 6.

7. Differential Scanning Calorimetry Data

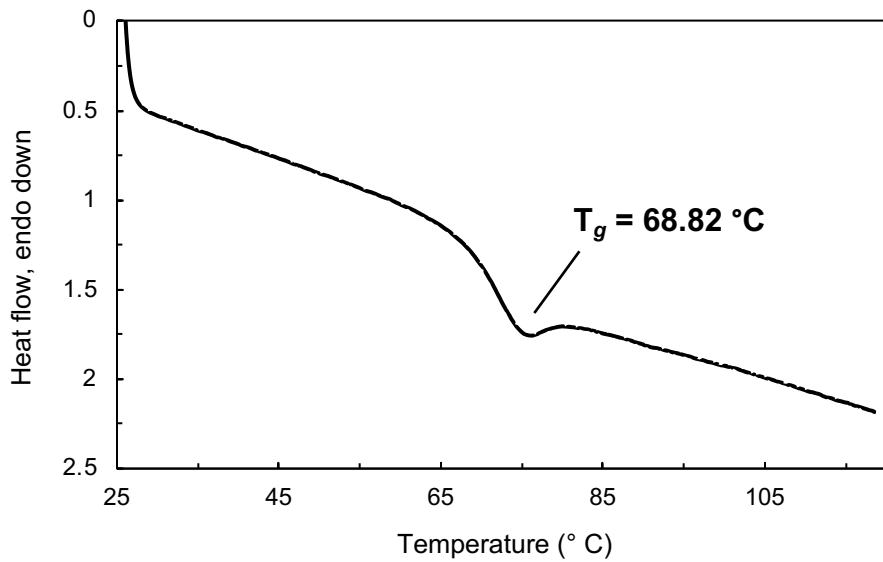


Fig. S47 DSC trace of CHO/CPMA-*r*-BO/CPMA from Table 2, Entry 1.

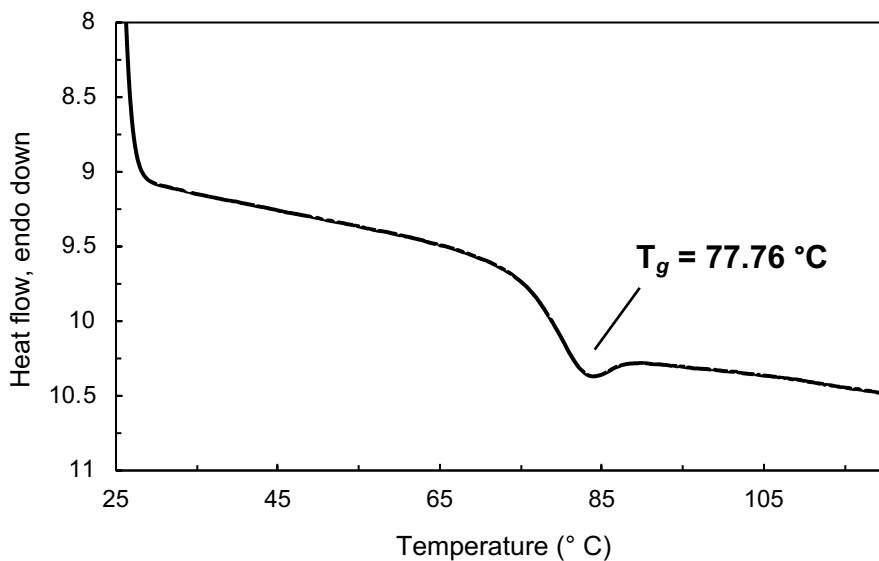


Fig. S48 DSC trace of CHO/CPMA-*r*-BO/CPMA from Table 2, Entry 2.

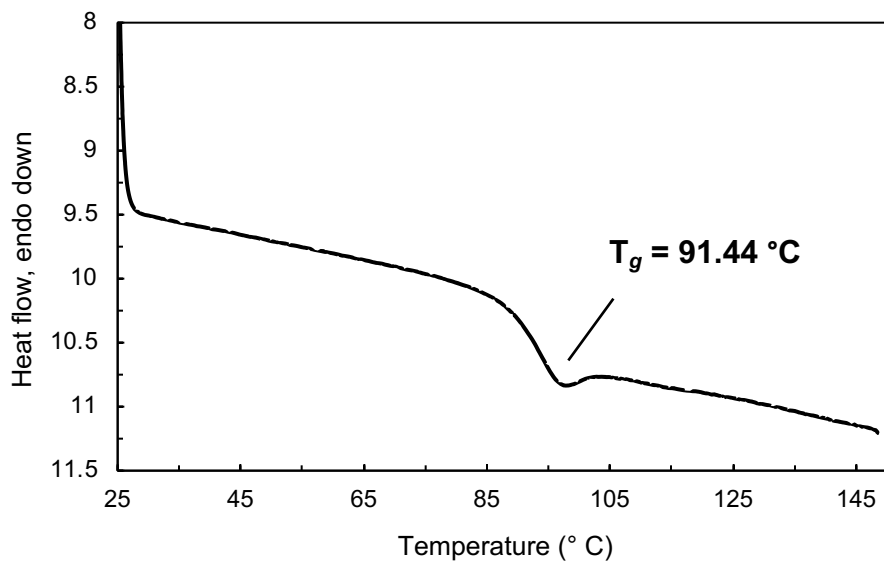


Fig. S49 DSC trace of CHO/CPMA-*r*-BO/CPMA from Table 2, Entry 3.

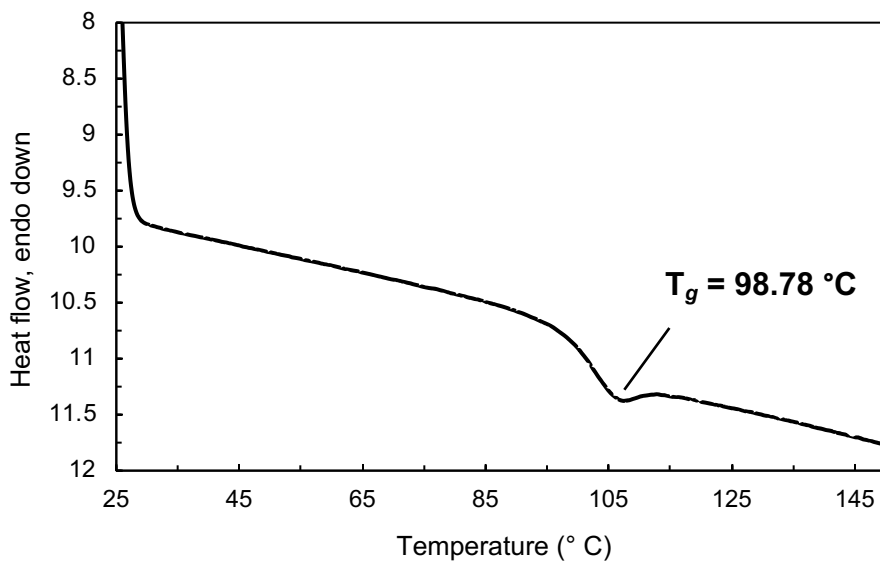


Fig. S50 DSC trace of CHO/CPMA-*r*-BO/CPMA from Table 2, Entry 4.

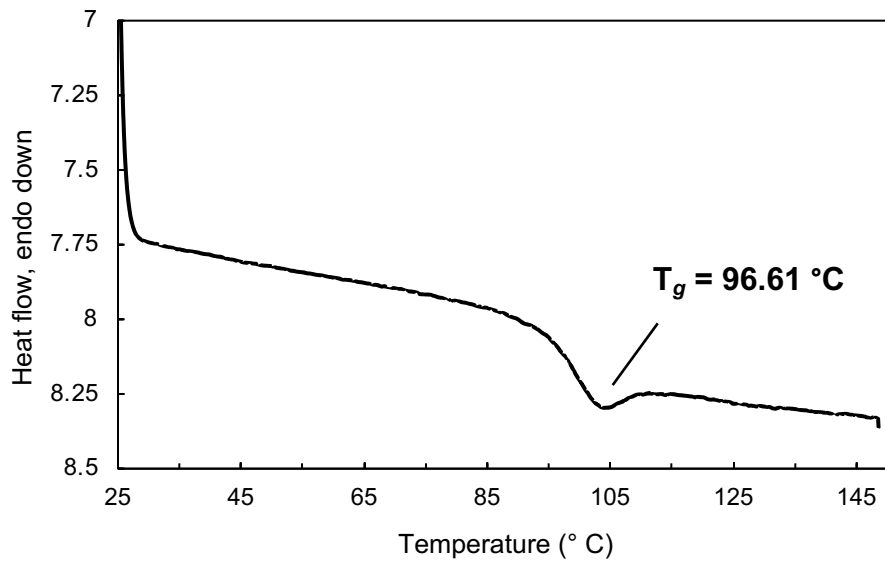


Fig. S51 DSC trace of CHO/CPMA-*r*-BO/CPMA from Table 2, Entry 5.

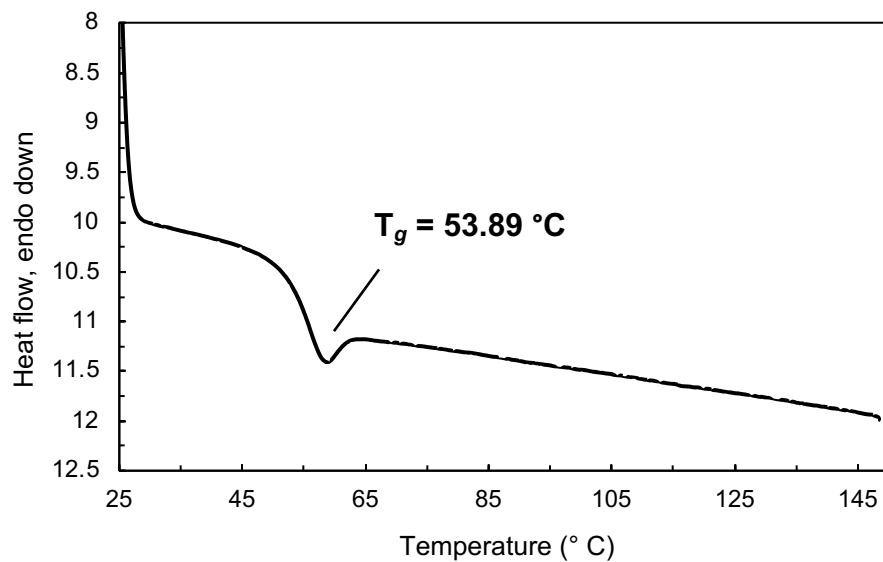


Fig. S52 DSC trace of BO/CPMA from Table S4, Entry 1.

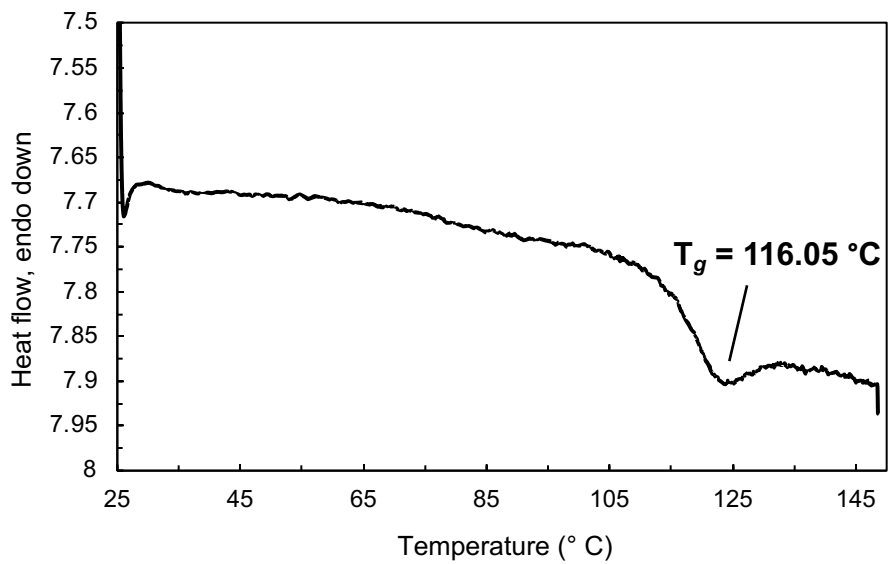


Fig. S53 DSC trace of CHO/CPMA from Table S4, Entry 7.

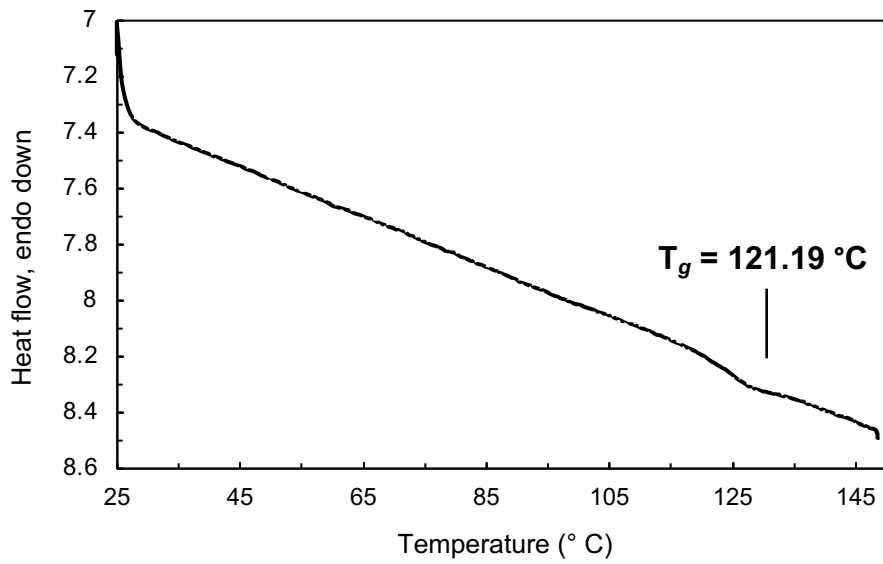


Fig. S54 DSC trace of CHO/PA-*b*-CHO/CPMA from Table S5, Entry 1.

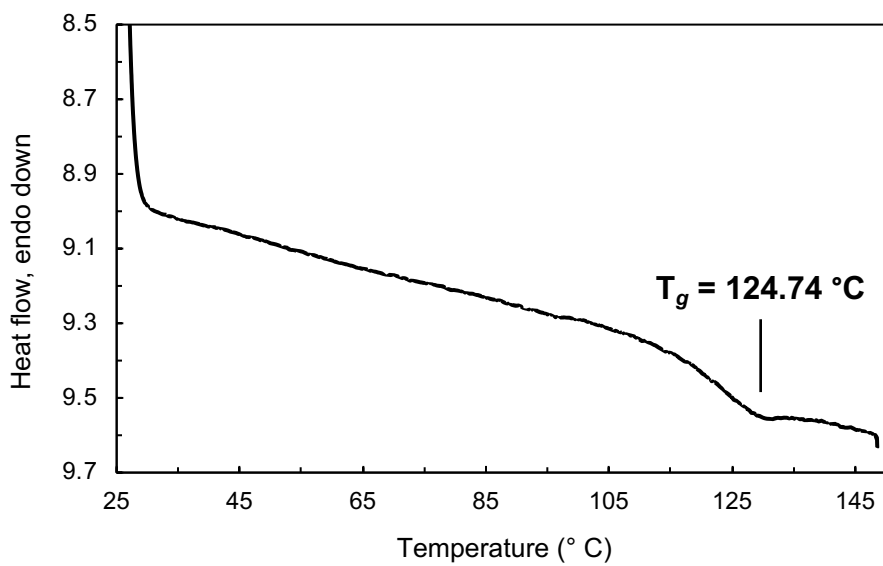


Fig. S55 DSC trace of CHO/PA-*b*-CHO/CPMA from Table S5, Entry 2.

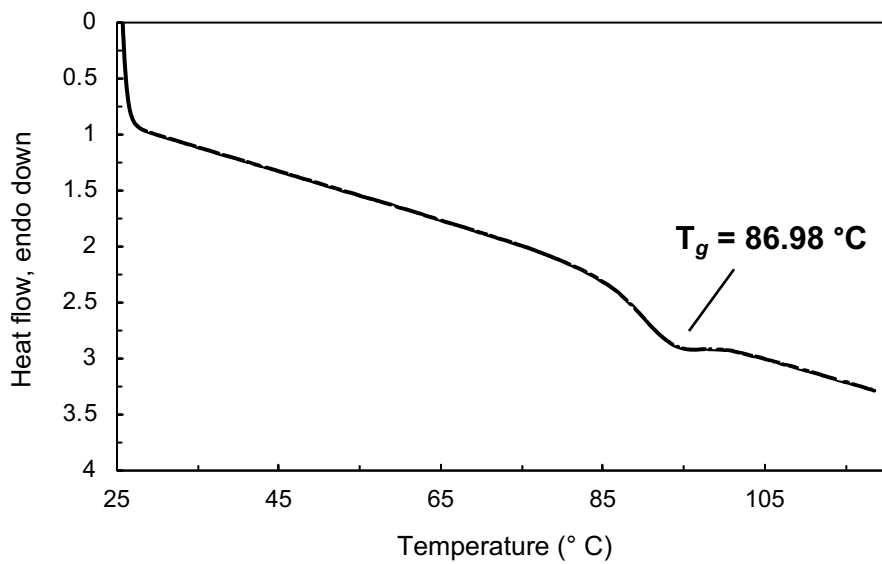


Fig. S56 DSC trace of CHO/GA-*r*-CHO/CPMA from Table S5, Entry 3.

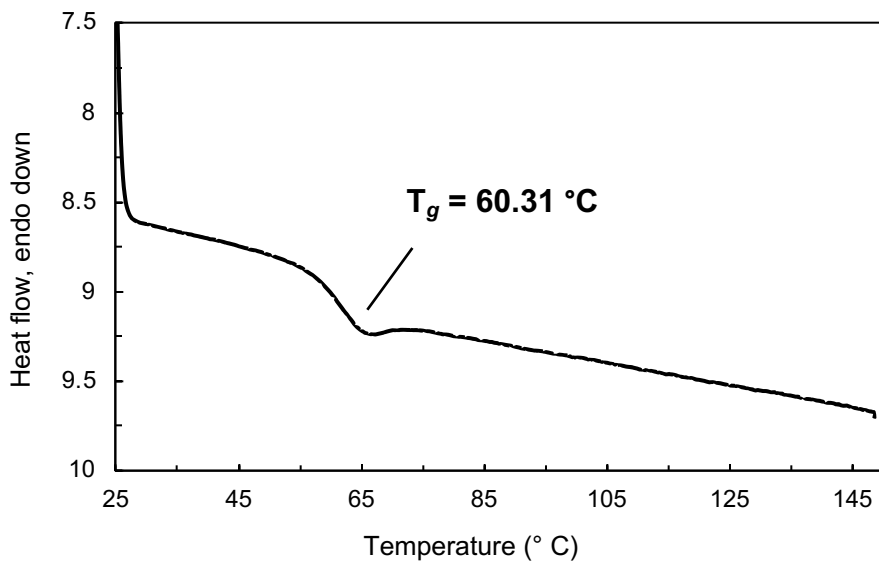


Fig. S57 DSC trace of CHO/GA-r-CHO/CPMA from Table S5, Entry 4.

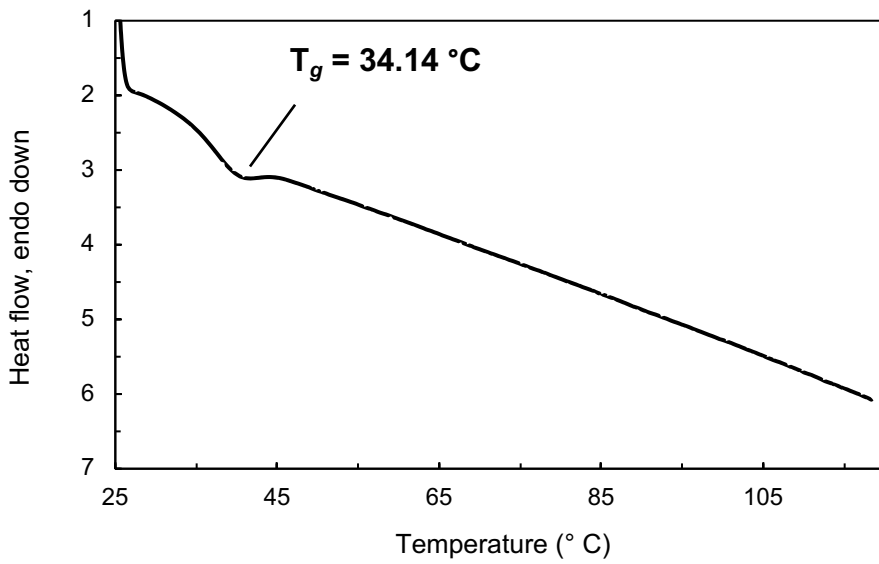


Fig. S58 DSC trace of CHO/GA-r-CHO/CPMA from Table S5, Entry 5.

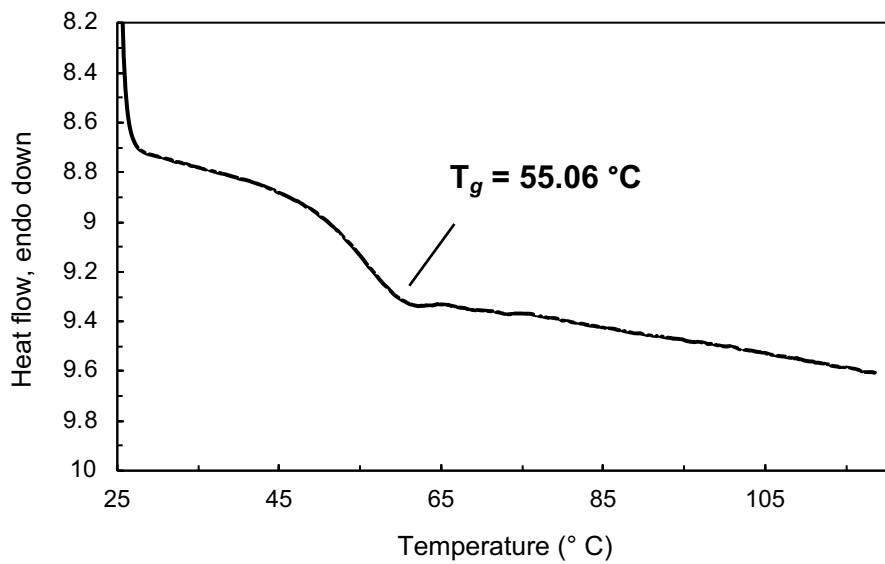


Fig. S59 DSC trace of CHO/GA-*r*-CHO/PA from Table S5, Entry 6.

8. Reactivity Ratios

8.1 Calculation of reactivity ratios

Due to the rate-determining step of the ROCOP of epoxides and cyclic anhydrides involving only epoxide ring opening, turn-over frequency data from individual ROCOP reactions does not allow accurate predictions of polymer sequence in the presence of multiple anhydrides. Therefore, a nonterminal compositional drift copolymerization kinetics model was employed to determine the reactivity ratios of multiple anhydride pairs.⁴⁻⁶ Following the experimental procedure described in section 2.1, Equations 3 and 4 were used to calculate reactivity ratios of a mixture of two anhydrides. For these equations, p_A and p_B are the respective conversions of A and B monomer with $p_A = 1 - (A(t)/A_0)$. The calculated reactivity ratios are then fit to the experimental data as shown in Fig. 4 of the manuscript and Fig S60.

$$p_{AB}(p_A) = 1 - n_A(1 - p_A) - (1 - n_A)(1 - p_A)^{r_B} \quad (3)$$

$$p_{AB}(p_B) = 1 - (1 - n_A)(1 - p_B) - n_A(1 - p_B)^{r_A} \quad (4)$$

8.2 Additional reactivity ratio plots

The reactivity ratios of most monomer pairs are reported in the main text, and the order of reactivity is highlighted at the end of Fig. 6. Below in Fig. S60 is two additional anhydride mixtures polymerized in the presence of CHO.

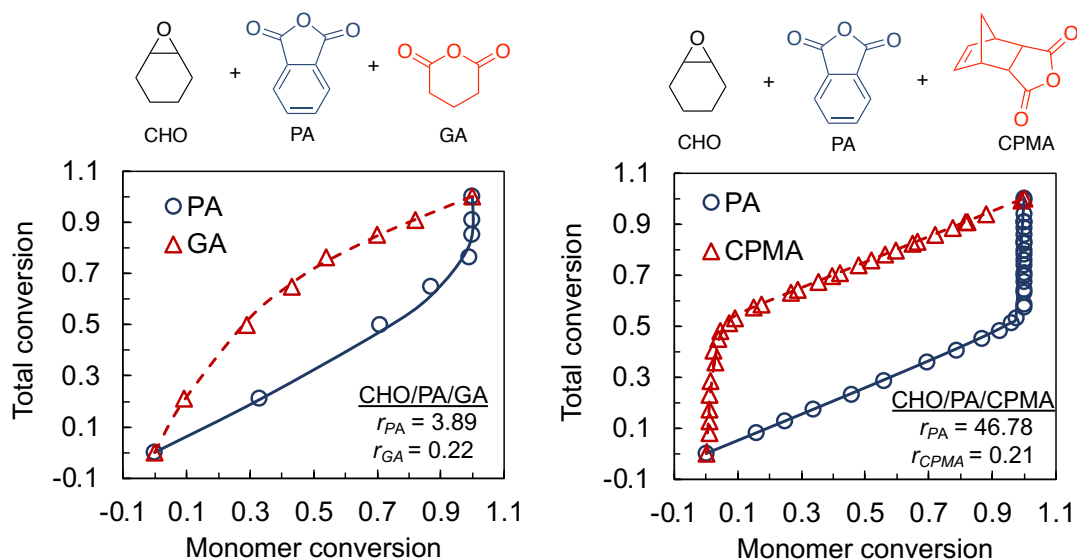


Fig. S60 Plot of CHO/PA/GA and CHO/PA/CPMA consumption in the presence of CHO.

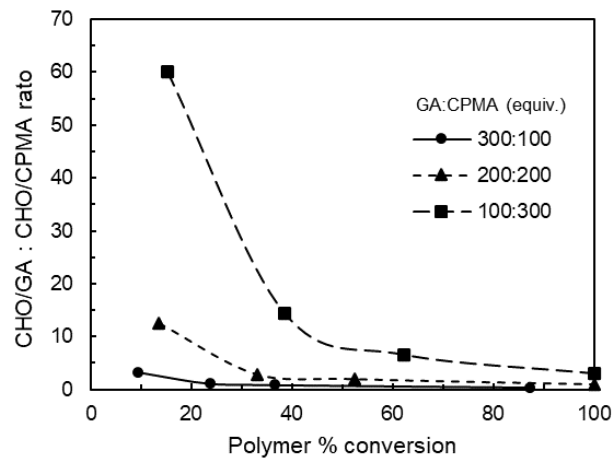


Fig. S61 Plot of % incorporation of CHO/GA vs. CHO/CPMA in varying GA:CPMA feed ratio equivalence.

8.3 Data for Epoxide Mixtures

As described in the manuscript, the Mayo-Lewis equation can be used to predict copolymer sequence for mixtures of epoxide in the presence of one anhydride. For this to be true, two assumptions must be met: the polymerization must follow nonterminal polymerization kinetics, and that the initial monomer feed ratio remains relatively unchanged. When two competing epoxides are present, the epoxide ring opening (ERO) is also the rate determining step (RDS), which suggests that the observed rate of each separate polymerization of monomer pairs should inform the polymer sequence that is achieved. Additionally, support that the epoxide feed ratio isn't changing drastically enough to influence the reactivity ratios, Fig. S62 is a plot of BO and CHO conversion in the presence of PA (from the ^1H NMRs of Fig. S7). This linear plot is also highlighted in Fig. 6 of the main text.

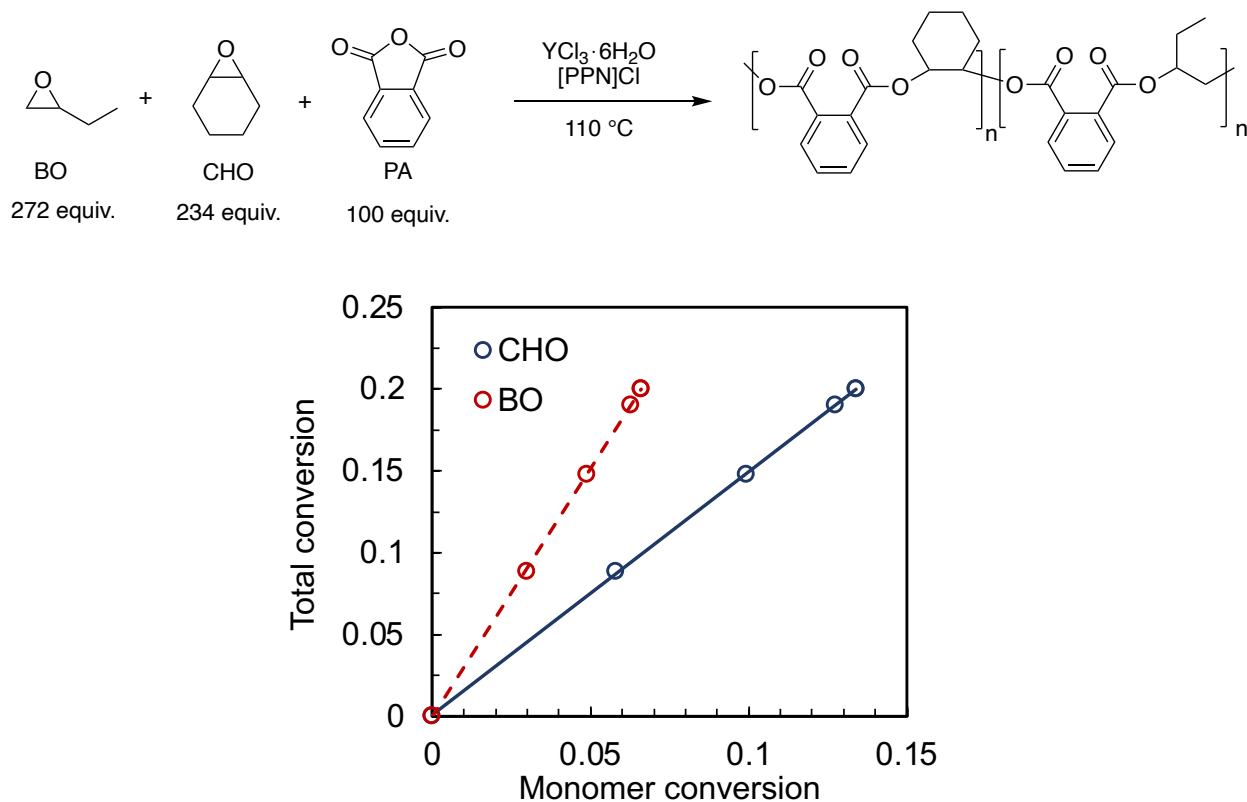


Fig. S62 Plot of CHO and BO conversion (x-axis) against total epoxide conversion (y-axis) for the ROCOP of BO/PA and CHO/PA.

9. References

- 1.** M. E. Fieser, M. J. Sanford, L. A. Mitchell, C. R. Dunbar, M. Mandal, N. J. V. Zee, D. M. Urness, C. J. Cramer, G. W. Coates and W. B. Tolman, *J. Am. Chem. Soc.*, 2017, **139**, 15222 – 15231.
- 2.** S. Hoops, S. Sahle, R. Gauges, C. Lee, J. Pahle, N. Simus, M. Singhal, L. Xu, P. Mendes and U. Kummer, *Bioinformatics*, 2006, **22**, 3067.
- 3.** B. Han, L. Zhang, B. Liu, X. Dong, I. Kim, Z. Duan and P. Theato, *Macromolecules*, 2015, **48**, 3431 – 3437.
- 4.** X. Xia, R. Suzuki, T. Gao, T. Isono and T. Satoh, *Nat. Comm.*, 2022, **13**, 163.
- 5.** B. S. Beckingham, G. E. Sanoja, N. A Lynd, *Macromolecules*, 2015, **48**, 6922 – 6930.
- 6.** M. Chwatko, N. A. Lynd. *Macromolecules*, 2017, **50**, 2714 – 2723.